

# Development of Oxadiazole-Sulfonamide-Based Compounds as Potential Antibacterial Agents

Asghar Ali,<sup>○</sup> Phool Hasan,<sup>○</sup> Mohammad Irfan, Amad Uddin, Ashba Khan, Juhi Saraswat, Ronan Maguire, Kevin Kavanagh, Rajan Patel, Mukesh C. Joshi, Amir Azam, Mohd. Mohsin, Qazi Mohd. Rizwanul Haque,\* and Mohammad Abid\*



Cite This: *ACS Omega* 2021, 6, 27798–27813



Read Online

ACCESS |



Metrics & More

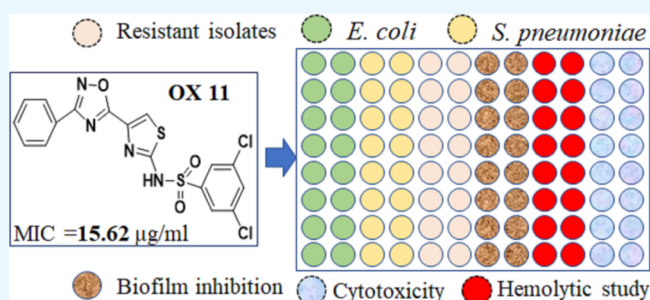


Article Recommendations



Supporting Information

**ABSTRACT:** In this work, substituted 1,2,4-oxadiazoles (OX1–OX27) were screened against five bacterial strains, identified to be OX7 and OX11 as growth inhibitors with minimum inhibitory concentration (MIC) values of 31.25 and 15.75  $\mu\text{g}/\text{mL}$ , respectively. The growth inhibitory property of OX7 and OX11 was further validated by disk diffusion, growth curve, and time kill curve assays. Both disrupted biofilm formation with 92–100% reduction examined by the XTT assay were further visualized by scanning electron microscopy analysis. These compounds in combination with ciprofloxacin also exhibit synergy against *Escherichia coli* cells. With insignificant cytotoxic behavior on HEK293 cells, human red blood cells, and *Galleria mellonella* larvae, OX11 was tested against 28 multidrug resistant environmental isolates of bacteria and showed inhibition of *Kluyvera georgiana* and *Citrobacter werkmanii* strains with 32 and 16  $\mu\text{g}/\text{mL}$  MIC values, respectively. The synergistic behavior of OX11 with ampicillin showed many fold reductions in MIC values against *K. georgiana* and *Klebsiella pneumoniae* multidrug resistant strains. Further, transmission electron microscopy analysis of OX11-treated *E. coli* cells showed a significantly damaged cell wall, which resulted in the loss of integrity and cytosolic oozing. OX11 showed significant changes in the secondary structure of human serum albumin (HSA) in the presence of OX11, enhancing HSA stability. Overall, the study provided a suitable core for further synthetic alterations and development as an antibacterial agent.



## 1. INTRODUCTION

According to the 2016 UN Declaration on Antimicrobial Resistance, global strategies and campaigns are underway to combat the disease.<sup>1,2</sup> The availability of inadequate treatment and extensive use of antimicrobial agents has resulted in antimicrobial resistance against the available drugs.<sup>2</sup> Thus, the conspicuous absence of novel and effective antimicrobials to control the microbial growth and increasing resistance has encouraged us to develop novel antimicrobial entities. Among various factors, formation of a biofilm is one of the significant features adopted by bacteria to develop resistance toward antibiotics.<sup>3</sup> Antibiotic resistance in bacteria may increase due to formation of a biofilm, which can elevate the rate of infection and cause morbidity and thus is important in clinical illnesses. In the presence of certain antimicrobials, growth in planktonic cells is increased to several folds as compared to biofilm, demonstrated by the susceptibility data literature.<sup>4</sup> However, in most biofilm susceptibility studies, only the survival of cells in a preformed biofilm is recorded rather than the ability of a biofilm to grow. Several approaches have been identified for the search of efficient antimicrobials, which can disrupt biofilm formation, including the role of nitrogen containing heterocycles as a biofilm inhibitor/disruptor.<sup>5,6</sup>

Among them, oxadiazole, a five-membered azole, and its derivatives are best known for their wide spectrum of antimicrobial activity. Oxadiazole ring containing compounds have been discovered and studied for their various properties *viz.* antitumor, antioxidant, antibacterial, antiviral, anti-inflammatory, insecticidal, and antiparasitic activities.<sup>7–19</sup> Besides enormous biological potential of oxadiazole derivatives, we preferred sulfonamide functionality with the aim to link it with the oxadiazoles to get anticipated improved antimicrobial motifs. Sulfonamides are well-known for their broad spectrum activity against Gram-positive and Gram-negative strains and also exhibit activity *viz.* carbonic anhydrase inhibition, insulin releasing, anti-tumor and anti-inflammatory effects, etc.<sup>20–23</sup> Based on the dominant biological profile of oxadiazoles as well as sulfonamides, we screened our library of diversely substituted oxadiazoles (OX1–OX27) against five

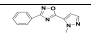
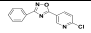
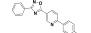
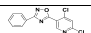
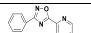
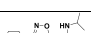
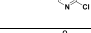
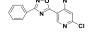
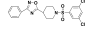
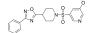
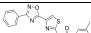
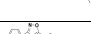

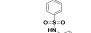
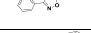
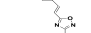
Received: June 28, 2021

Accepted: September 30, 2021

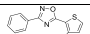

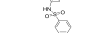
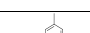
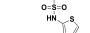
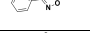
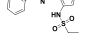
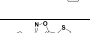
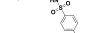
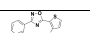

Published: October 14, 2021



Table 1. MIC Values (in  $\mu\text{g/mL}$ ) of all the Screened Compounds<sup>a</sup>

S. No.	Compound name	Compound Structure	<i>P. aeruginosa</i>	<i>E. coli</i>	<i>S. pneumoniae</i>	<i>S. typhimurium</i>	<i>E. faecalis</i>
1.	OX-1		>500	250	500	>500	>500
2.	OX-2		>500	125	500	>500	>500
3.	OX-3		500	500	250	>500	>500
4.	OX-4		>500	>500	>500	>500	>500
5.	OX-5		>500	500	250	>500	>500
6.	OX-6		250	125	250	>500	>500
7.	<b>OX-7</b>		31.25	15.62	15.62	>500	>500
8.	OX-8		125	62.5	>500	>500	>500
9.	OX-9		>500	500	500	>500	>500
10.	OX-10		>500	>500	500	>500	>500
11.	<b>OX-11</b>		15.62	15.62	15.62	>500	>500
12.	OX-12		>500	500	>500	250	>500
13.	OX-13		250	125	>500	>500	>500
14.	OX-14		>500	>500	>500	>500	>500
15.	OX-15		>500	>500	500	250	>500
16.	OX-16		250	125	>500	>500	>500

<sup>a</sup>CIP, ciprofloxacin; AMP, ampicillin.

S. No.	Compound name	Compound Structure	<i>P. aeruginosa</i>	<i>E. coli</i>	<i>S. pneumoniae</i>	<i>S. typhimurium</i>	<i>E. faecalis</i>
17.	OX-17		500	>500	>500	>500	>500
18.	OX-18		>500	>500	>500	>500	>500
19.	OX-19		250	250	500	>500	>500
20.	OX-20		500	>500	250	>500	>500
21.	OX-21		500	500	>500	>500	>500
22.	OX-22		>500	500	250	>500	>500
23.	OX-23		500	500	250	500	>500
24.	OX-24		250	>500	500	>500	500
25.	OX-25		>500	>500	>500	>500	>500
26.	OX-26		>500	250	500	>500	>500
27.	OX-27		250	250	500	500	500
28.	<b>CIP</b>	-	0.48	0.24	0.24	0.97	15.62
29.	<b>AMP</b>	-	15.62	15.62	31.25	>500	62.5

tested bacterial strains. Among all, **OX7** and **OX11** showed better potency against *Streptococcus pneumoniae*, *Pseudomonas aeruginosa*, and *Escherichia coli*. Furthermore, growth kinetic as well as time kill curve studies were done on *E. coli* and *S. pneumoniae* treated with **OX7** and **OX11** confirming bactericidal character. Interestingly, both the compounds almost eradicated the formation of the biofilm in *E. coli* cells. Further, **OX11** was studied for *in vitro* (cytotoxicity assays and hemolysis) and *in vivo* toxicity assays on *Galleria mellonella* larvae and revealed to be non-toxic. The effect of **OX11** on resistant bacterial strains showed that it is a selective inhibitor of *Kluyvera georgiana* and *Citrobacter werkmanii* with a 32  $\mu\text{g/mL}$  MIC value. The antibacterial efficacy of **OX11** was considerably improved when it was combined with AMP against *S. pneumoniae* and *K. georgiana*.

Further, the interactions between human serum albumin (HSA) and **OX11** were also studied. HSA has the ability to bind remarkably to a variety of drugs and impacts its delivery and efficacy. Mostly, concentration of an unbound drug in a tissue depends completely on the presence of an unbound drug in the plasma.<sup>24</sup> The interaction of the HSA drug has become increasingly important to analyze the pharmacological as well

as the pharmacokinetic effect of a drug.<sup>25–28</sup> Various spectroscopic techniques *viz.* UV–visible, fluorescence, 3D fluorescence, synchronous fluorescence, and circular dichroism (CD) were employed, and the experimental results suggested that **OX11** strongly quenches the intrinsic fluorophore of HSA. The thermodynamic parameters *viz.*  $\Delta H$ ,  $\Delta S$ , and  $\Delta G$  suggest the involvement of the hydrophobic interaction and spontaneity of the **OX11**-HSA complex formation. Additionally, synchronous fluorescence showed that amino acid tryptophan (Trp) is involved in the quenching process. Circular dichroism (CD) data and three-dimensional (3D) fluorescence revealed that **OX11** stimulates the conformational changes in the secondary structure of HSA and enhances its stability.

## 2. RESULTS

**2.1. In Vitro Antibacterial Screening. 2.1.1. Minimum Inhibitory Concentration (MIC) Determination.** Preliminary antimicrobial screening of oxadiazole derivatives (**OX1**–**OX27**) resulted in **OX7** and **OX11** with better antibacterial activity against tested bacterial strains, and the data is presented in Table 1. **OX7** showed a MIC value of 31.25

$\mu\text{g/mL}$  against *P. aeruginosa* and  $15.75 \mu\text{g/mL}$  against *E. coli*, whereas **OX11** exhibited an MIC value of  $15.75 \mu\text{g/mL}$  against *P. aeruginosa* and *E. coli* (Table 1). Both compounds inhibited *S. pneumoniae* with an MIC value of  $15.75 \mu\text{g/mL}$ . However, no growth inhibition was observed against *Salmonella typhimurium* and *Enterococcus faecalis* with MIC values more than  $500 \mu\text{g/mL}$ . Thus, it was concluded from the study that **OX7** and **OX11** are selective inhibitors of *P. aeruginosa*, *S. pneumoniae*, and *E. coli* bacterial cells with a better growth inhibitory property.

**2.1.2. Disk Diffusion Assay.** The antibacterial efficacies of the test compounds **OX7** and **OX11** were determined using the disk diffusion assay on a solid nutritional agar medium at concentrations corresponding to  $1/2$ MIC, MIC, and 2MIC. The zones of clearance (dose-dependent) were observed in the assay when various concentrations of both test compounds were applied. On treatment with **OX7**, clear zone of inhibition (ZOI) values of 20, 23, and 24 mm were observed around the disk of  $1/2$ MIC, MIC, and 2MIC, respectively, with the culture of Gram-negative *E. coli* and the same result was observed with the culture of Gram-positive *S. pneumoniae* cells, whereas the ZOI values with the culture of Gram-negative *P. aeruginosa* were 19 mm ( $1/2$ MIC), 22 mm (MIC), and 23 mm (2MIC) (Table 2). On treatment with **OX11** the ZOI values obtained

**Table 2. Zone of Inhibition (ZOI) in mm Determined around the Disk of Various Concentrations of Compounds OX7 and OX11**

compound	bacterial strain	ZOI at distinct concentrations of the test compound		
		$1/2$ MIC	MIC	2MIC
<b>OX7</b>	<i>P. aeruginosa</i>	19 mm	22 mm	23 mm
	<i>S. pneumoniae</i>	20 mm	23 mm	24 mm
	<i>E. coli</i>	20 mm	23 mm	24 mm
<b>OX11</b>	<i>P. aeruginosa</i>	19 mm	22 mm	23 mm
	<i>S. pneumoniae</i>	19 mm	22 mm	25 mm
	<i>E. coli</i>	20 mm	22 mm	28 mm

were 20, 22, and 28 mm with *E. coli*; 19, 22, and 25 mm with *S. pneumoniae*; and 19, 22, and 23 mm with *P. aeruginosa* around the disk of  $1/2$ MIC, MIC, and 2MIC, respectively. Therefore, the largest ZOI is obtained with *S. pneumoniae* and *E. coli* against both the compounds. The images of agar plates showing zone of inhibition are provided in the Supporting Information.

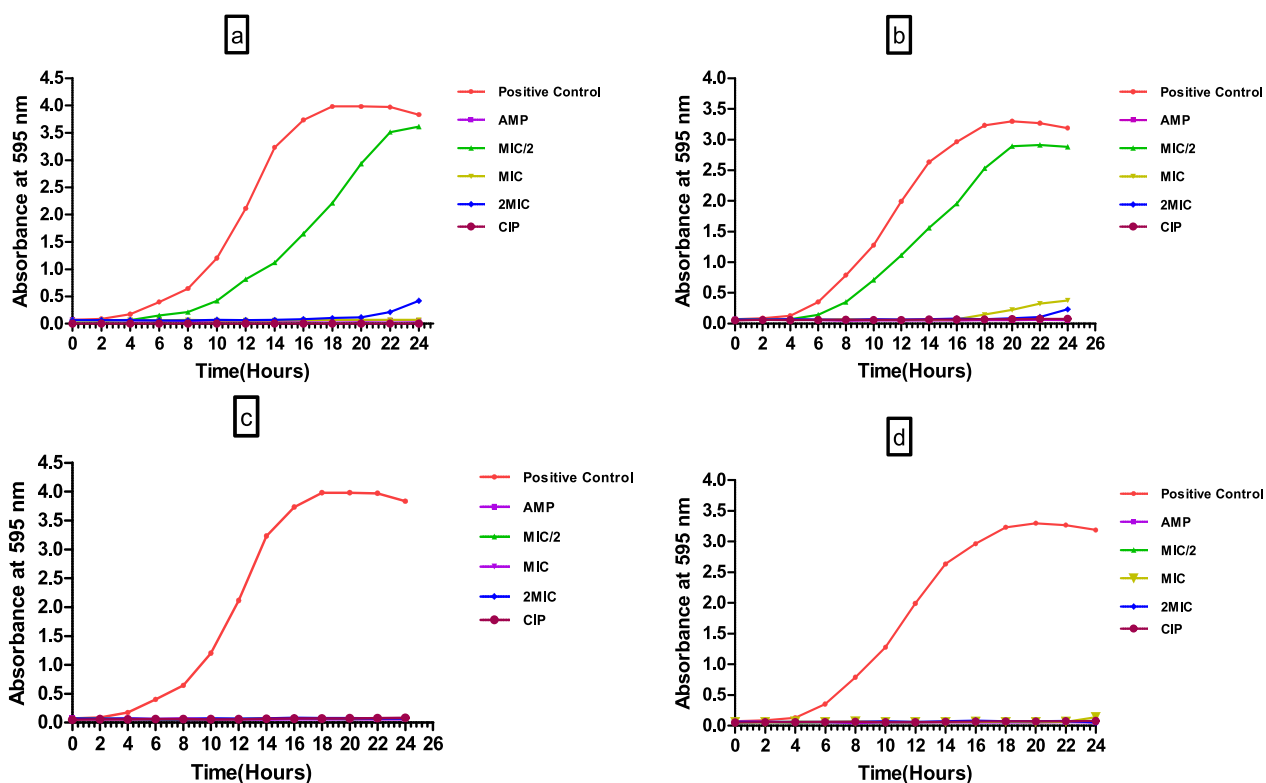
**2.1.3. Growth Kinetics Assay.** The effect of **OX7** and **OX11** on the growth of the test organisms was investigated by growth curve analysis using *E. coli* and *S. pneumoniae* bacterial strains. As a negative and a positive control, we took treated (CIP and AMP) cells and untreated cells, respectively. The result of the growth curve revealed an S-shape sigmoid curve for untreated bacterial cells. No growth was observed till 20 h in *E. coli* at 2 MIC and MIC of the test compound **OX7**. At  $1/2$ MIC of **OX7**, the growth of *E. coli* cells was observed after 4 h in comparison to untreated cells; it was still delayed. However, **OX11** completely prevented the growth of both strains of bacteria at all test concentrations. As a consequence, the data indicated that both compounds have antimicrobial effects against the tested strains. The study concluded that **OX11** is a more efficient inhibitor of the tested bacterial strains than **OX7** since no significant growth was detected at any of the test concentrations after 24 h (Figure 1).

**2.1.4. Time Kill Curve Study.** To establish whether the tested compounds are bactericidal or bacteriostatic in nature, a time kill curve study was conducted. The study was done at 4MIC and MIC concentrations of **OX7** and **OX11** against bacterial strains of *E. coli* and *S. pneumoniae* bacterial strains. The study demonstrated that there was only a slight difference in CFU (colony forming units) values for MIC and 4MIC concentrations. The killing activity was observed up to 24 h through a regular decrease in CFU with time intervals, which fallen up to  $<1 \log_{10}$  CFU. At the MIC concentration, there was a substantial drop in  $\log_{10}$  CFU/mL with time; however, no full eradication of the bacterial population was observed. At higher concentration, corresponding to 4MIC, significant eradication of tested bacterial cells was observed after 24 h. The observations explicitly indicated the bactericidal nature of both the test compounds against the tested bacterial strains (Figure 2a,b).

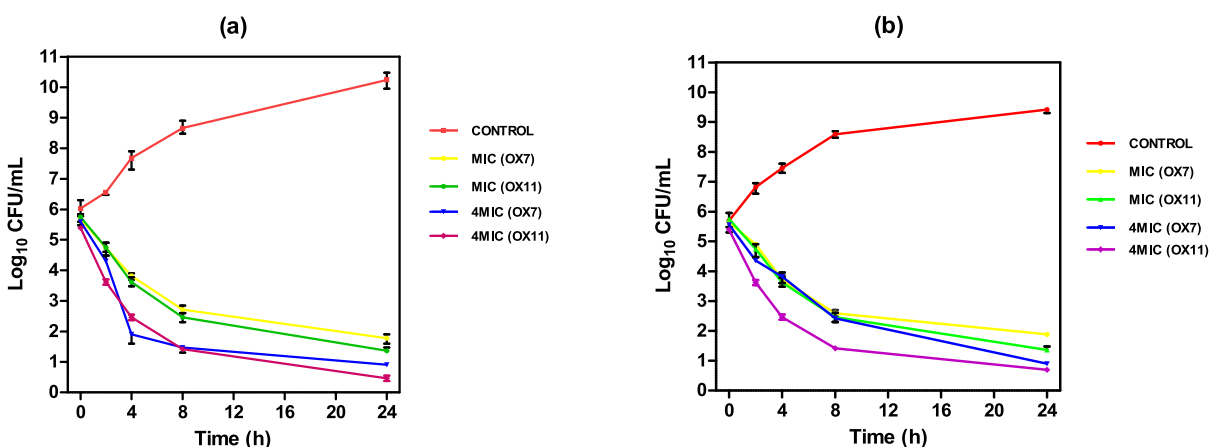
**2.1.5. Synergistic Antibacterial Activity of Test Compounds (OX7 and OX11).** To investigate the synergistic antibacterial activity, the selected compounds **OX7** and **OX11** were further evaluated in combination with CIP and AMP against *S. pneumoniae* and *E. coli* bacterial cells. The outcomes indicated a significant enhancement in the antibacterial activity of **OX7** against the *E. coli* strain when used in combination with CIP or AMP, showing synergy, but in the case of *S. pneumoniae*, it was an indifferent mode of interaction with combination of CIP, whereas a synergetic mode of interaction was observed with AMP. Similarly, **OX11** also showed synergy with CIP or AMP against *E. coli*. Additionally, **OX11** exhibits an indifferent mode of interaction with CIP and a synergistic mode of interaction with AMP against *S. pneumoniae*. The FICI value was  $1 < \text{FICI} \leq 4$  in all the combinations (Table 3). FICI indices of  $\leq 0.5$  and  $> 4$  were used to categorize synergy and antagonism, respectively, whereas  $1 < \text{FICI} \leq 4$  was used to indicate indifference.<sup>29</sup>

**2.2. Assessment of Biofilm Disruption.** **2.2.1. XTT (2,3-Bis(2-methoxy-4-nitro-5-sulphophenyl)-2H-tetrazolium-5-carboxanilide) Assay.** Biofilm formation is a significantly important virulence factor of bacterial pathogens, which helps them to survive in stressed conditions within the host. The effect of **OX7** and **OX11** on biofilm disruption was evaluated in *E. coli* and *S. pneumoniae* bacterial strains using an XTT assay kit. Both the compounds showed significant disruption of biofilm formation in *E. coli* as well as in *S. pneumoniae*. Compound **OX7** disrupted 92, 86, and 84% biofilm formation in *E. coli* in the presence of 4MIC, 2MIC, and MIC concentrations, respectively. In the case of *S. pneumoniae*, it disrupted 98, 95, and 92% biofilm formation at their 4MIC, 2MIC, and MIC concentrations, respectively. Similarly, compound **OX11** disrupted 95, 90, and 81% of biofilm formation in *E. coli* at their 4MIC, 2MIC, and MIC concentrations, respectively, while completely disrupting biofilm formation at each concentration in *S. pneumoniae*. Thus, compounds **OX7** and **OX11** exert their antibacterial effect via disruption of biofilm formation (Figure 3).

**2.2.2. Scanning Electron Microscopic (SEM) Analysis.** The XTT test was used to detect biofilm disruption in *E. coli* cells, and the results were quantified using scanning electron microscopy (SEM). The concentrations of the 2MIC value of **OX7** and **OX11** were taken to study their effectiveness against biofilm development as compared to untreated cells. The cells in untreated samples appeared clustered and entrenched in the extracellular matrix under SEM analysis



**Figure 1.** Growth curve analysis of (a) *E. coli* in the presence of distinct concentration of OX7, (b) *S. pneumoniae* in the presence of distinct concentration of OX7, (c) *E. coli* in the presence of distinct concentration of OX11, and (d) *S. pneumoniae* in the presence of various concentrations of OX11.



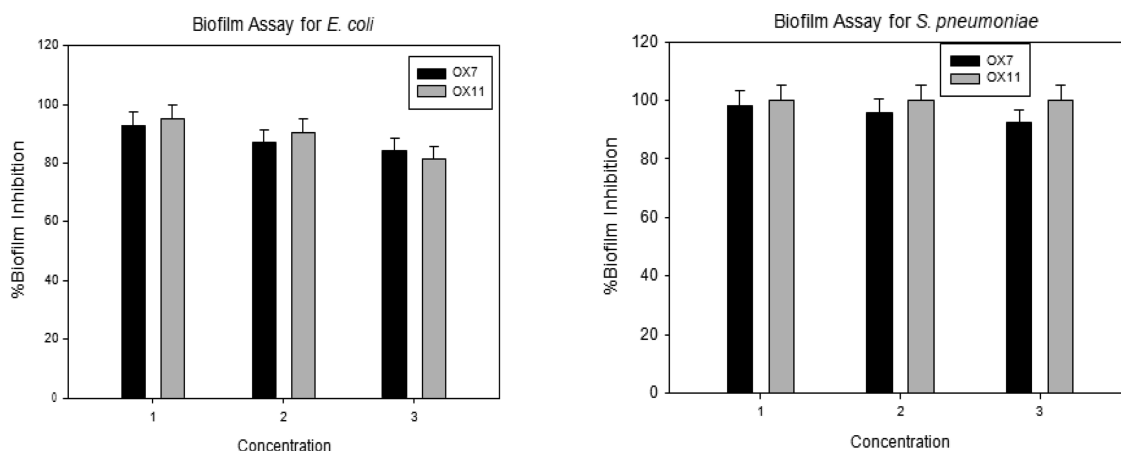
**Figure 2.** Time kill curve for (a) *E. coli* and (b) *S. pneumoniae* treated with OX7 and OX11 at different concentrations.

**Table 3. Antibacterial Activity of OX7 and OX11 in Combination with CIP and AMP**

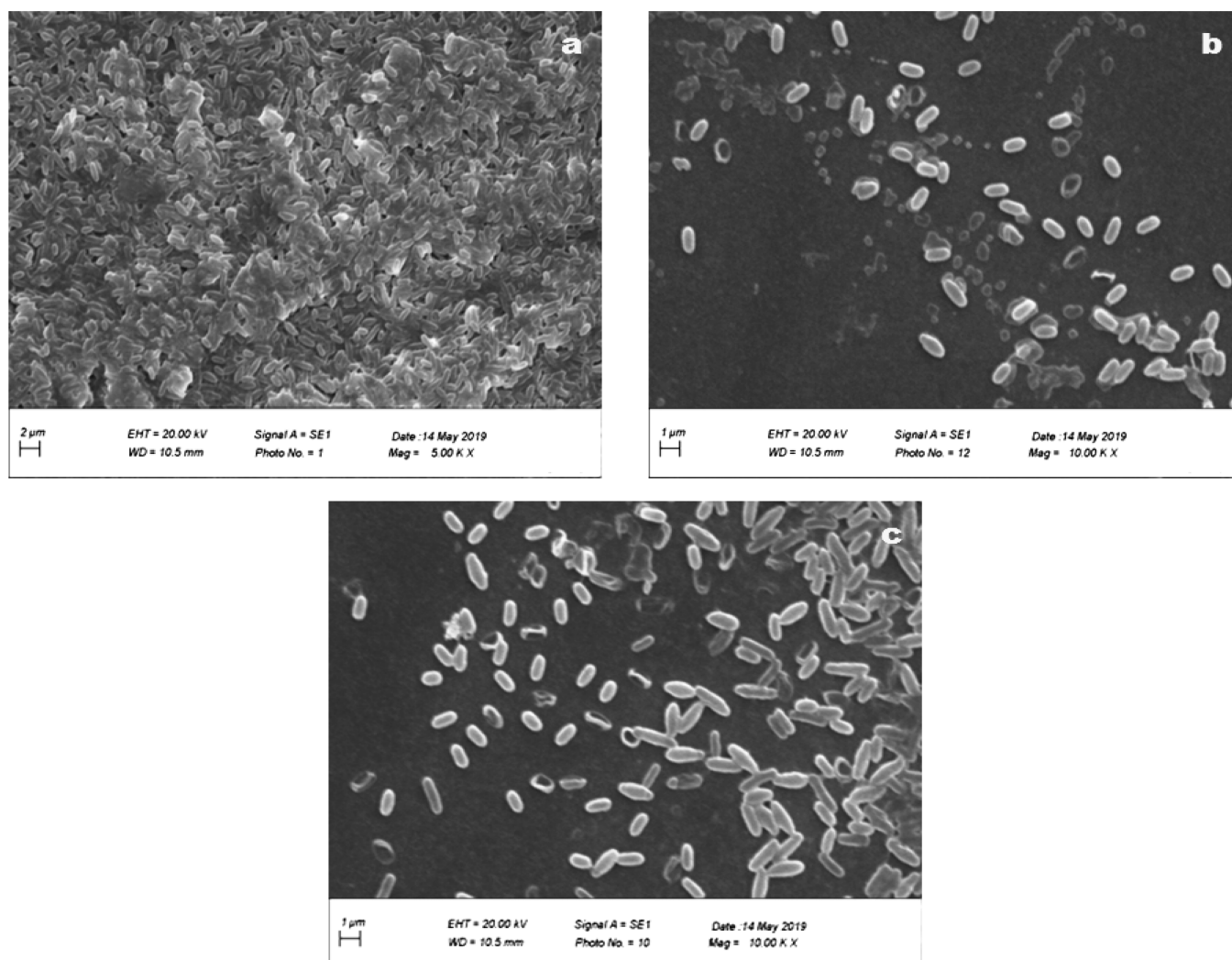
combination	bacterial strain	MIC alone ( $\mu\text{g/mL}$ )				MIC in combination ( $\mu\text{g/mL}$ )				FICI <sup>a</sup>	interaction pattern
		OX7	OX11	CIP	AMP	OX7	OX11	CIP	AMP		
OX7 with CIP	<i>E. coli</i>	16		0.25		2		0.062		0.375	synergistic
	<i>S. pneumoniae</i>	16		0.25		2		0.5		2.125	indifferent
OX7 with AMP	<i>E. coli</i>	16			16	0.5			0.078	0.343	synergistic
	<i>S. pneumoniae</i>	16			31.25	1			2.5	0.1425	synergistic
OX11 with CIP	<i>E. coli</i>		16	0.25			2	0.062		0.375	synergistic
	<i>S. pneumoniae</i>		16	0.25			2	0.25		1.125	indifferent
OX11 with AMP	<i>E. coli</i>		16		16		0.5		0.078	0.03	synergistic
	<i>S. pneumoniae</i>		16		31.25		0.25		0.312	0.025	synergistic

<sup>a</sup>Fractional inhibitory concentration index.





**Figure 3.** Percent biofilm disruption by the XTT assay in *E. coli* and *S. pneumoniae* corresponding to (1) 4MIC, (2) 2MIC, and (3) MIC concentrations of OX and OX11.



**Figure 4.** SEM images of biofilm formation in (a) untreated *E. coli* cells, (b) OX11-treated *E. coli* cells, and (c) OX7-treated *E. coli* cells.

(Figure 4a). At 2MIC, the sample showed significant damage in biofilm (Figure 4b,c). The result clearly indicated that, in comparison with the untreated cells, both the test compounds disrupted the formation of biofilm in *E. coli* cells, but it was also observed that the effect was stronger in the case of OX11. Thus, we concluded that OX11 has the better ability to disrupt

biofilm formation and its molecular mechanism can be further evaluated in this regard.

**2.3. Toxicological Studies.** 2.3.1. Hemolytic Assay. A hemolytic assay using human red blood cells (hRBCs) was used to screen any toxic effect of the test compounds (OX7 and OX11). The findings were compared to the conventional

antibiotic CIP. Compounds OX7 and OX11 demonstrated 36 and 38% hemolysis of *hRBCs*, respectively, at a concentration of 400  $\mu\text{g/mL}$ . At the same concentration, however, standard drug CIP showed 28% hemolysis. Our test compounds were likewise found to be non-toxic at concentrations between 25 and 12.5  $\mu\text{g/mL}$ , indicating their non-toxic nature. Both the test compounds demonstrated less than 10% hemolysis, indicating their non-toxic character (Figure 5).

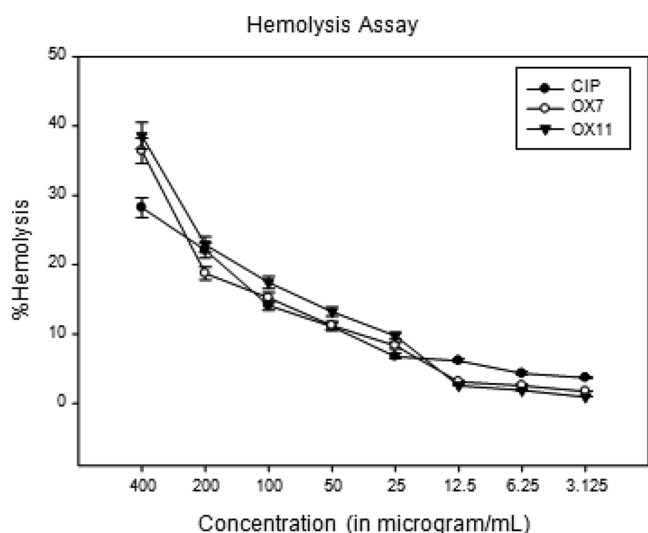


Figure 5. Hemolytic activity of compounds OX, OX11, and CIP on human red blood cells (*hRBCs*).

2.3.2. *MTT (3-(4,5-Dimethylthiazol-2-yl)-2,5-diphenyl tetrazolium bromide) Assay*. To be further sure about the non-toxic behavior of the test compounds, we evaluated the cytotoxic effect of the compounds on human embryonic kidney (HEK293) cells as the test model to check the cell viability. The screening was carried out for 48 h using the MTT assay in the concentration range of 0–250  $\mu\text{M}$ . It was interesting to find that, even at 250  $\mu\text{M}$  concentration of OX7 and OX11, the viability of HEK293 cells remained unaffected (Figure 6). These findings indicated that both compounds are

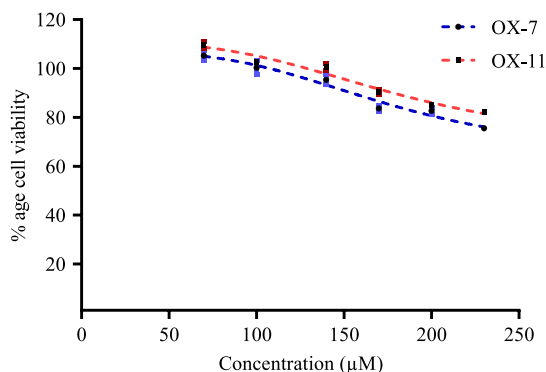


Figure 6. Cytotoxic effect of OX and OX11 using HEK293 cells.

non-toxic to HEK293 cells at the concentration ranges tested. Furthermore, based on the cell survivability tests, we can speculate that, among the two lead test compounds, OX11 may be taken as a promising lead molecule against selective bacterial strains since it did not induce harm to normal cells in the micromolar concentration levels tested but rather inhibited

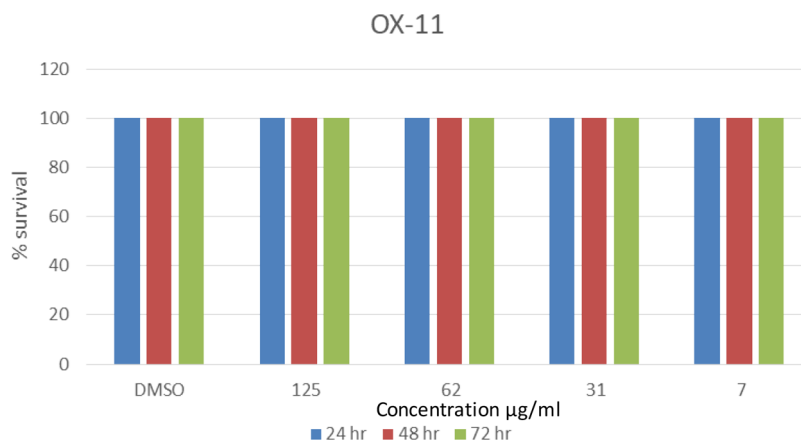
bacterial cells. So, based on the toxicity assays also, OX11 emerged as the lead compound as it was observed in the case of other biological assays.

2.3.3. *Evaluation of In Vivo Toxicity of OX11 on G. mellonella Larvae*. To further evaluate the cytotoxic effect of our lead compound, we used *G. mellonella* as the model that exhibits strong correlation with the innate immunity response of mammals. An *in vivo* administration of 125  $\mu\text{g/mL}$  for the test compound (OX11) did not induce any significant change in the larval viability, indicating its nontoxic behavior toward the larvae (Figure 7). However, hemocyte density of the larvae shows some variation, which is indicative of a stress response in larvae (Figure 8).

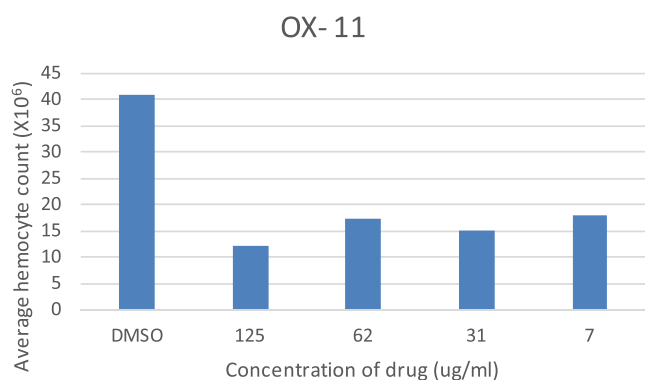
2.4. *Transmission Electron Microscopic (TEM) Analysis*. To assess the impact of OX11 on the morphology of *E. coli* cells, TEM analysis was performed. We used the *E. coli* cell culture treated with the MIC concentration of OX11 and untreated cells as a control. The treated cells had moderate to severe cellular abnormalities, but the untreated cells were normal in shape with undamaged cell walls (Figure 9). The treatment of bacterial cells with OX11 resulted in a substantial loss of cell wall integrity and cytoplasmic oozing. The degraded cell walls of bacteria observed in the TEM micrographs propose the bactericidal activity of OX11.

2.5. *Confocal Laser Scanning Microscopic (CLSM) Analysis*. Using confocal laser microscopy, the cellular uptake of compound OX11 by *E. coli* bacterial cells was determined. The bacterial cells were stained with DAPI (4',6-diamidino-2-phenylindole), a nucleic acid binding dye. DAPI is a fluorescent dye that binds strongly to the DNA's A-T rich region and emits blue fluorescence as emission spectra at 461 nm after being excited at 358 nm. Untreated as well as treated cells (exposed to MIC of OX11 for 3 h) were stained and observed under confocal laser microscopy. Untreated cells were alive and did not emit blue fluorescence, as shown in Figure 10a. In the treated sample, the number of live cells decreases (Figure 10b). The presence of compound OX11 resulted in a large number of fluorescence emitting cells, clearly indicating cell lysis. As a result of this finding, it was determined that compound OX11 has significant antibacterial properties, which could be investigated further to develop better antibacterial agents.

2.6. *Effect of the Lead Compound (OX11) on Resistant Strains*. 2.6.1. *MIC Determination*. Based on the biological assays performed on both the selected compounds, OX11 was carried forward to further investigate its inhibitory effect on environmental resistant strains in terms of MIC against 19 different strains of *E. coli*, two strains of *Klebsiella pneumoniae*, and one each of *Acinetobacter*, *K. georgiana*, and *C. werkmanii*. All these strains were isolated from environmental wastewater samples from Delhi-NCR.<sup>30,31</sup> The MIC values were calculated and compared to AMP and SMX as the reference antibacterial drugs. The results showed that OX11 exhibited better results than AMP against *K. georgiana* (with an MIC value of 32  $\mu\text{g/mL}$ ) and *C. werkmanii* (with an MIC value of 32  $\mu\text{g/mL}$ ) (Table 4). This MIC value is far less than as compared with that of the standard drug AMP (MIC, 500  $\mu\text{g/mL}$ ) in the case of *K. georgiana* strain. With SMX (MIC value,  $\sim$ 1000  $\mu\text{g/mL}$ ), OX11 showed better result against *E. coli* strain (AE-31) also, in addition to *K. georgiana* and *C. werkmanii*. Therefore, we found that OX11 is more effective than SMX as the MIC values of the former are far less than



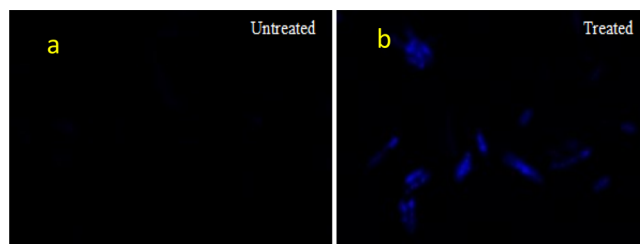
**Figure 7.** Survival of *G. mellonella* larvae injected with OX11 over 72 h at 30 °C.



**Figure 8.** Changes in hemocyte density following injection with OX11 over 72 h at 37 °C.

those of the latter against selective resistant bacterial strains, rendering it a promising antibacterial agent.

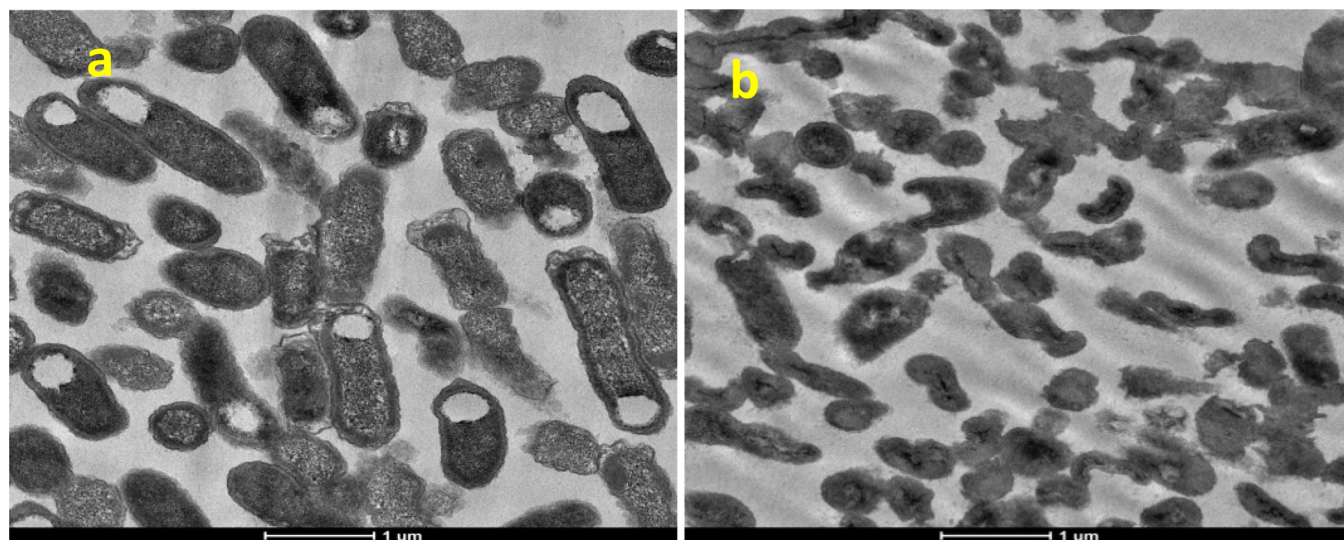
**2.6.2. Combination Studies of OX11 against Selective Environmental Bacterial Isolates.** The combination study of OX11 was performed with the standard drugs SMX and AMP as per the standard protocol. The results showed the synergistic effect of OX11 with SMX against KP, SH-14, AE-44 (FICI value, 0.282), and SH-52 (FICI value, 0.314).



**Figure 10.** Confocal laser microscopic images of *E. coli* cells (a) untreated and (b) treated with OX11 at MIC concentrations.

Meanwhile, in combination with AMP, OX11 showed synergy with KP, EH-8, and SH-14 (FICI value range between 0.032 and 0.314) (Table 5). An FICI value of less than 0.5 is considered to be in synergy. The combination studies proved that OX11 has effectively exhibited synergy against a wide range of resistant bacterial strains in combination with AMP and SMX.

**2.7. HSA Binding Studies.** The interaction between HSA and OX11 was studied using UV-vis, steady state fluorescence, synchronous, 3D fluorescence, and CD spectroscopy techniques. These results provide accurate insights regarding the binding of OX11 with HSA.<sup>32</sup> The



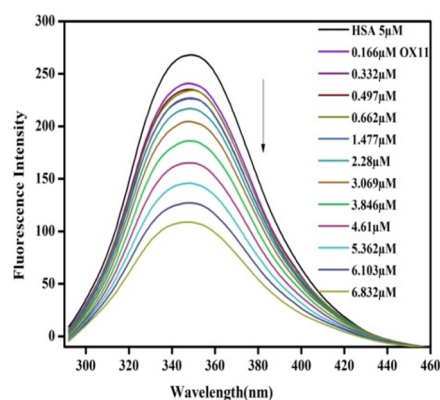
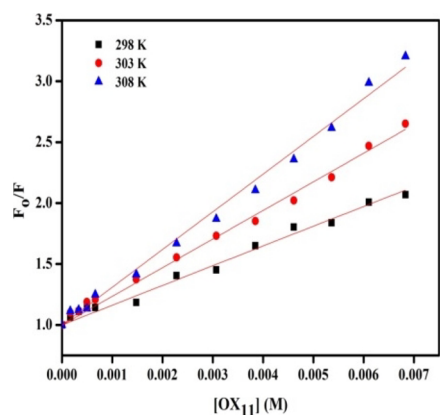
**Figure 9.** TEM images of (a) untreated *E. coli* cells and (b) OX11-treated *E. coli* cells.



**Table 4. MIC Values of OX11 against Environmental Isolates of Bacteria ( $\mu\text{g/mL}$ )**

bacterial isolates code	strain	OX11	AMP	SMX
AE-9	<i>E. coli</i>	1000	1000	>1000
AE-27	<i>E. coli</i>	1000	1000	1000
AE-44	<i>E. coli</i>	1000	500	1000
AE-32	<i>E. coli</i>	1000	>1000	>1000
AE-17	<i>E. coli</i>	1000	1000	500
AE-23	<i>E. coli</i>	1000	1000	500
AE-42	<i>E. coli</i>	1000	1000	>1000
AE-21	<i>E. coli</i>	>1000	1000	>1000
AE-31	<i>E. coli</i>	500	8	>1000
EC-36	<i>E. coli</i>	1000	1000	1000
EC-2	<i>E. coli</i>	1000	500	1000
EC-3	<i>E. coli</i>	1000	1000	1000
EC-6	<i>E. coli</i>	1000	1000	1000
EC-25	<i>E. coli</i>	1000	500	1000
OB-18	<i>E. coli</i>	1000	1000	1000
OB-6	<i>E. coli</i>	1000	500	>1000
AE-2	<i>E. coli</i>	1000	500	1000
OE-11	<i>E. coli</i>	1000	500	>1000
EE-2	<i>E. coli</i>	1000	500	>1000
EH-8	<i>Acinetobacter</i> sp.	1000	32	1000
KP	<i>K. pneumoniae</i>	1000	1000	1000
EA-13	<i>K. pneumoniae</i>	>1000	125	>1000
SH-14	<i>K. georgiana</i>	32	500	500
SH-52	<i>C. werkmanii</i>	32	8	500

fluorescence spectra of HSA in the absence and presence of OX11 were noted, as shown in Figure 11. The maximum fluorescence emission was observed at 353 nm, which is a characteristic peak of the Trp residue in HSA. The fluorescence intensity was found to be decreasing with the addition of a higher concentration of OX11, and the process is referred as the quenching process (Figures 12 and 13). The quenching constant was calculated using a Stern–Volmer equation (eq 4) at different temperatures, and the values are listed in Table 6. From Table 6, the increasing value of  $K_{sv}$  with increasing temperature suggests the involvement of dynamic quenching. The values of the different thermodynamic parameters, such as enthalpy change ( $H$ ), entropy change ( $S$ ), and Gibbs free energy change ( $G$ ), are also determined using eqs 6 and 7, and the values are listed in Table 6. The

**Figure 11.** Fluorescence emission spectra of HSA ( $5 \mu\text{M}$ ) in the absence and presence of varied concentrations of OX11 at 298 K and pH 7.4.**Figure 12.** Stern–Volmer plot for the quenching of HSA by OX11 at 298, 303, and 308 K and pH 7.4.

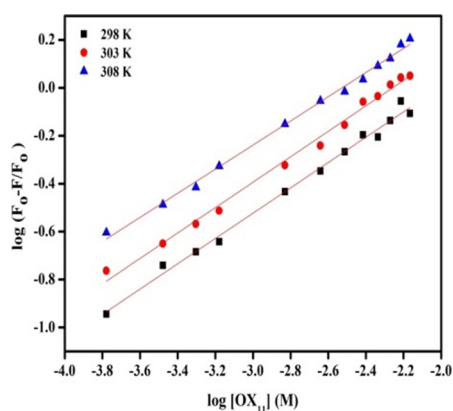
positive sign of  $\Delta S$  and  $\Delta H$  suggests the involvement of the hydrophobic interaction prevailing between the HSA and OX11 according to the Ross and Subramanian theory.<sup>33</sup> Further, the binding constant ( $K_b$ ) was calculated using a Van't Hoff plot (Figure 14), and the values are summarized in Table 6. The value of  $K_b$  showed an increase with temperature, which suggests that, at higher temperature, the complex formed between HSA and OX11 is strong. Also, the value of  $\Delta G$  was found to be negative, which showed that its interaction process

**Table 5. Antibacterial Activity of OX11 in Combination with SMX and AMP**

combinationn	bacterial strain	MIC alone ( $\mu\text{g/mL}$ )			MIC in combination ( $\mu\text{g/mL}$ )			FICI <sup>a</sup>	interaction pattern
		OX11	SMX	AMP	OX11	SMX	AMP		
OX11 with SMX	<i>Acinetobacter</i> sp. (EH-8)	1000	1000		500	32		0.532	indifferent
	<i>K. pneumoniae</i> (KP)	1000	1000		250	32		0.282	synergistic
	<i>K. georgiana</i> (SH-14)	32	500		8	16		0.282	synergistic
	<i>C. werkmanii</i> (SH-52)	32	500		8	32		0.314	synergistic
	<i>E. coli</i> (AE-44)	1000	1000		250	32		0.282	synergistic
	<i>E. coli</i> (AE-23)	1000	500		1000	32		1.064	indifferent
OX11 with AMP	<i>Acinetobacter</i> sp. (EH-8)	1000		32	62.5		4	0.187	synergistic
	<i>K. pneumoniae</i> (KP)	1000		1000	31.25		1	0.032	synergistic
	<i>K. georgiana</i> (SH-14)	32		500	8		32	0.314	synergistic
	<i>C. werkmanii</i> (SH-52)	32		8	16		2	0.750	indifferent
	<i>E. coli</i> (AE-44)	1000		500	500		16	0.532	indifferent
	<i>E. coli</i> (AE-23)	1000		500	500		32	0.564	indifferent

<sup>a</sup>Fractional inhibitory concentration index.

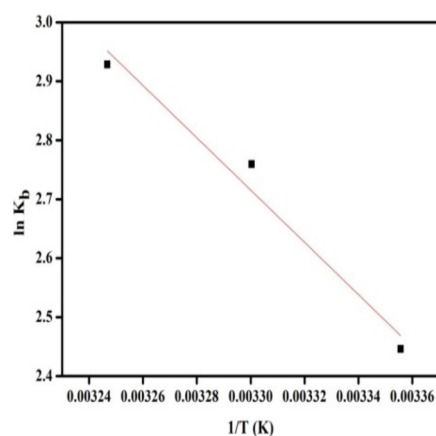




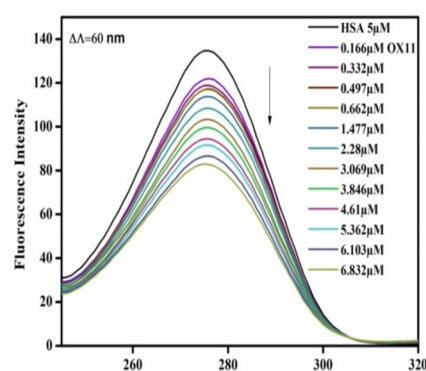
**Figure 13.** Double log plot for the quenching of HSA by OX11 at 298, 303, and 308 K and pH 7.4.

is spontaneous in nature.<sup>34</sup> In addition, the synchronous spectra were also recorded to determine the involvement of the residue in the quenching process. Figures 15 and 16 show the synchronous fluorescence spectra at  $\Delta\lambda = 60$  and 15 nm, which clarify the involvement of Trp and Tyr, respectively.<sup>35</sup> The synchronous results shown in Figures 15 and 16 suggest that, with the increasing concentration of OX11, the quenching of Trp was much stronger than the quenching of Tyr, which depicts that the quenching of HSA is mainly because of the involvement of the Trp residue. Also, the three-dimensional fluorescence spectra of the HSA and HSA-OX11 complex were recorded, as shown in Figure 17. The spectra revealed three distinct peaks. Peak 1 corresponds to Raleigh scattering, whereas peak 2 corresponds to the presence of tyrosine and tryptophan residue, and peak 3 is the characteristic peak of the polypeptide backbone structure. From Figure 17, it was observed that OX11 quenched the fluorescence intensity of peaks 2 and 3 of HSA alone dropped from 132.78 to 118.22 and 153.05 to 97.71, respectively, whereas in the presence of OX11, peaks 2 and 3 decreased from 65.07 to 1 and 107.03 to 90, respectively (Table 7). The decrease in stock shift suggests the binding between HSA and OX11, which was also established by our steady state fluorescence results. The decrease in fluorescence intensity of both peaks is evident of a conformational change occurring in the HSA molecule in the presence of OX11.<sup>36</sup>

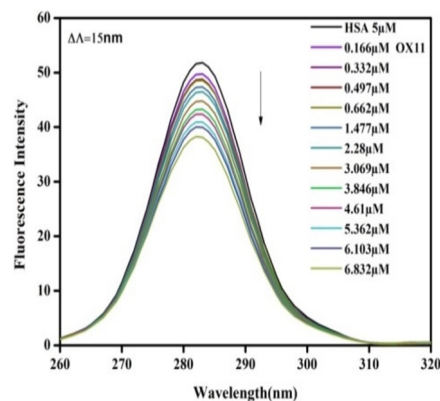
In addition, the complexation was further confirmed by UV-vis spectroscopy. The UV-vis spectra of pure HSA are shown in Figure 18, where a strong band at 278 nm provides the information about the buried aromatic amino acids (Trp, Tyr, and Phe). Figure 18 shows the continuous decrease in the maximum absorbance on the addition of increasing concentration of OX11, which signifies the complex formation between HSA and OX11. Further, absorption spectra were used to calculate the value of the binding constant using the double reciprocal plot (as shown in Figure 19) using eq 3. The value of the binding constant was in the same order and was in



**Figure 14.** Vant't Hoff plot for the quenching of HSA by OX11 at 298 K and pH 7.4.



**Figure 15.** Synchronous fluorescence spectra of HSA ( $5 \mu\text{M}$ ) in the absence and presence of varied concentrations of OX11 at  $\Delta\lambda = 60$  nm at 298 K and 7.4 pH.



**Figure 16.** Synchronous fluorescence spectra of HSA ( $5 \mu\text{M}$ ) in the absence and presence of varied concentrations of OX11 at  $\Delta\lambda = 15$  nm at 298 K and pH 7.4.

good agreement with the result obtained from fluorescence spectroscopy.<sup>37</sup> Additionally, a significant change in the value

**Table 6. Binding Parameters and Thermodynamic Parameters of HSA-OX11 Using Fluorescence Spectroscopy**

temp (K)	$K_{sv}$ (L/mol)	$K_b$ (L/mol)	$n$	$R^2$	$\Delta H$ (kJ/mol)	$\Delta S$ (kJ mol <sup>-1</sup> K <sup>-1</sup> )	$\Delta G$ (kJ/mol)
298	162.08	11.55	0.62	0.996	36.86	144.16	-6.09
303	234.98	15.79	0.66	0.996			-6.81
308	309.54	18.70	0.69	0.997			-7.53

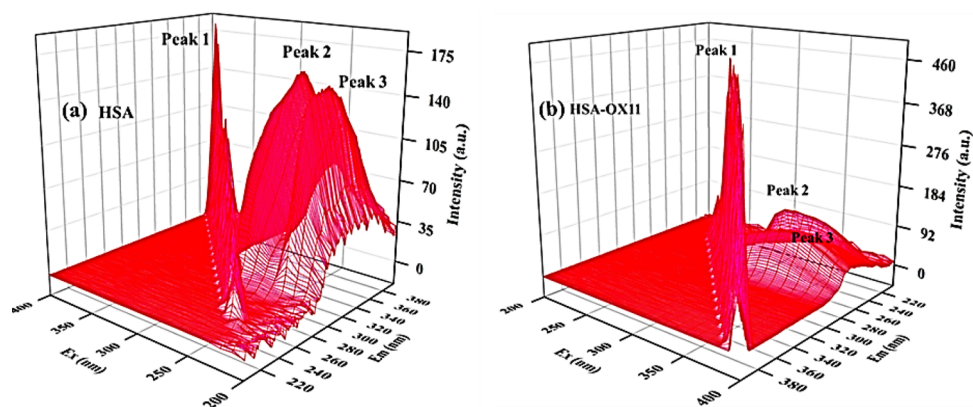


Figure 17. Three-dimensional fluorescence spectra of the (a) HSA ( $5 \mu\text{M}$ ) and (b) HSA-OX11 complex.

Table 7. Parameters of the 3D Fluorescence of the HSA and HSA-OX11 Complex

	HSA		HSA-OX11	
	peak 2	peak 3	peak 2	peak 3
peak position	280/345.07	230/337.03	280/279.06	230/320
relative intensity	132.78	153.05	118.22	97.71
$\Delta\lambda$ (nm)	65.07	107.03	1	90

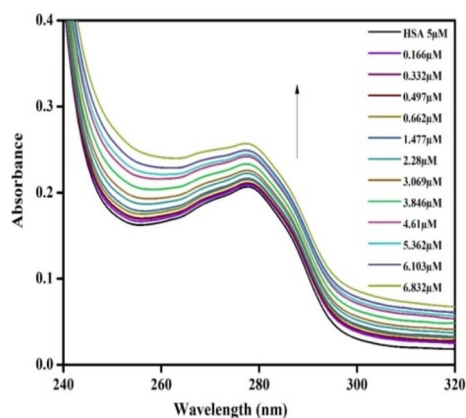


Figure 18. UV-vis spectra of HSA ( $5 \mu\text{M}$ ) in the absence and presence of varied concentrations of OX11 at 298 K and pH 7.4.

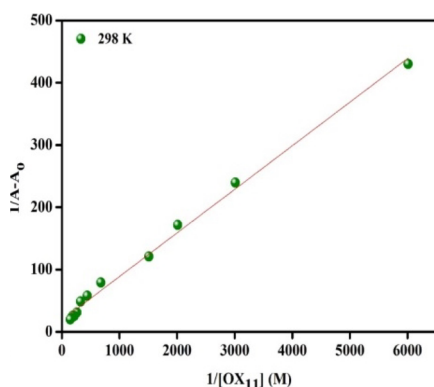


Figure 19. Double reciprocal plot for the UV-vis spectra of HSA ( $5 \mu\text{M}$ ) in the absence and presence of OX11 at 298 K and pH 7.4.

of the  $\alpha$ -helical content was observed from CD spectra (shown in Figure 20). At lower concentration, the value of the  $\alpha$ -helical content increased from 58.8 to 60.3% as compared to the

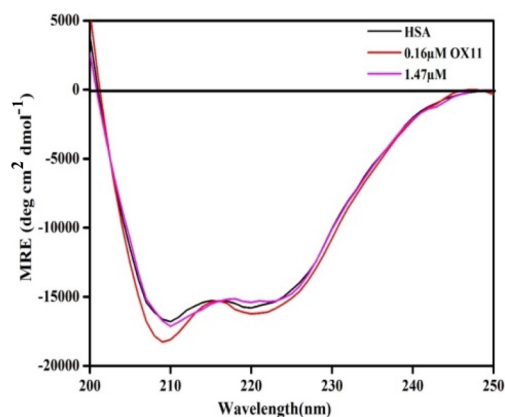


Figure 20. Far UV CD of HSA with OX11 at 298 K and pH 7.4.

native protein, whereas it decreased from 60.3 to almost 58.3% (toward native protein), which suggests the significant change in the secondary structure of HSA in the presence of OX11. A lower concentration of OX11 stabilized the secondary structure (movement to a more folded structure), whereas unfolding (folded to unfolded state) of HSA at a higher concentration of OX11 was seen.<sup>38</sup> The present study could play an important role in pharmacological applications of drug-protein complexation.

### 3. DISCUSSION

Bacterial infections remain a risk to public health despite the availability of antibiotics due to the rising level of the multidrug resistant bacteria.<sup>39,40</sup> Antibiotic resistance is one of the top 10 threats, according to the World Health Organization (WHO).<sup>41</sup> The Center for Disease Control and Prevention (CDC) predicted that a “post-antibiotic era” will begin soon.<sup>42</sup> Therefore, it is obvious for medical science researchers to find new ways to overcome the scarcity of effective antibacterial agents with better efficacy. In this intensive study, to develop a better antibacterial agent, we first synthesized a diverse series of oxadiazole-sulfonamide-based compounds (OX1–OX27), and through the preliminary screening, two compounds OX7 and OX11 were picked as selective inhibitors of *S. pneumoniae*, *P. aeruginosa*, and *E. coli* bacterial strains. The bactericidal action against the selected bacterial strains revealed through various antibacterial studies conducted on these two test compounds clearly suggests that the OX11 compound can be taken as the lead compound. Drugs that show synergy are always considered better than drugs that do not because by

counteracting biological compensation, sparing doses on each chemical, or utilizing context-specific multitarget processes, synergistic combinations of two or more pharmaceuticals can prevent toxicity and other side effects associated with high doses of single treatments.<sup>43–45</sup> We examined the antibacterial efficacy of compound **OX11** against 28 multidrug resistant strains (MDR) strains. Although our lead compound **OX11** is found to be indifferent toward *S. pneumoniae*-sensitive bacterial strain in combination with CIP, indeed, it shows synergy with CIP when tested against *E. coli* cells. Further, when tested in combination with AMP, the interaction pattern of **OX11** was found synergistic with the tested sensitive bacterial strains. Interestingly, **OX11** also showed synergy with AMP and SMX against 3 out of 28 MDR bacterial strains. The findings of the cell viability tests suggested that **OX11** could be used as a promising antibacterial agent against specific bacterial strains because it is non-toxic to mammalian cells but inhibits bacterial cells selectively. Moreover, the viability of *G. mellonella* larvae was not affected in an *in vivo* toxicity assay using **OX11** up to a dose of 125  $\mu\text{g}/\text{mL}$ , showing its nontoxic behavior toward the larvae. However, the hemocyte density of the larvae shows some variation, which is indicative of a stress response in larvae. Single cells (planktonic mode) and biofilms are two alternative “lifestyles” that bacteria can adopt. As the estimated 80% of all bacterial infections are biofilm-related,<sup>46,47</sup> we examined the effect of **OX7** and **OX11** on biofilm formation. We observed that both the test compounds emerge as a significant disruptor of biofilm formation, damaging its formation by up to 90%. Unfortunately, the molecular mechanism of biofilm disruption could not be elucidated. Our findings through confocal laser microscopy clearly show cell lysis due to the presence of **OX11**, confirming its significant antibacterial property, which indicates its potential as a better pharmacophore that may form the basis of further study. Binding of plasma protein plays an important role in drug disposition and its efficacy.<sup>48</sup> Human serum albumin (HSA) binds a diverse set of drugs, especially neutral and negatively charged hydrophobic compounds.<sup>49</sup> On binding with HSA, **OX11** was found to stabilize the secondary structure, forming a spontaneous and stable complex even at higher temperature.

#### 4. CONCLUSIONS

In summary, a series of oxadiazole-sulfonamide-based compounds bearing various substitutions were synthesized and screened as an effective antibacterial agent against a group of Gram-positive as well as Gram-negative strains. **OX7** and **OX11** emerged out as significant antibacterial compounds against sensitive strains like *S. pneumoniae*, *P. aeruginosa*, and *E. coli* strains, and **OX11** is moderately effective against MDR *K. georgiana* and *C. werkmanii* strains. Compound **OX11** exhibited a synergistic effect with AMP against the *Acinetobacter* isolate in addition to *K. pneumoniae* and *K. georgiana*. Compound **OX11** with SMX showed a synergistic effect against *C. werkmanii*, *E. coli*, *K. pneumoniae*, and *K. georgiana* strains. Further research revealed that growth kinetic analyses validated the bacteriocidal effect of the test compounds. The CLSM study indicated that **OX11** can be further explored as a better pharmacophore. The TEM study revealed that **OX11** exhibited considerable cell wall destruction and membrane rupture in *E. coli* bacterial cells, resulting in cell death. Furthermore, these compounds were found to be effective anti-biofilm agents in *E. coli* and to be non-cytotoxic

in the HEK293 cell line at concentrations of up to 250  $\mu\text{M}$ . **OX11**, on the other hand, showed modest change in hemocyte density, indicating a stress response, and was found to be safe to *G. mellonella* larvae up to a concentration of 125  $\mu\text{g}/\text{mL}$ . Our research suggests that the compound **OX11** would be further optimized to generate a more effective and safer antibacterial agent.

#### 5. MATERIALS AND METHODS

**5.1. Chemistry.** All the oxadiazole-based compounds bearing various substitutions (**OX1–OX27**) were synthesized and recently reported by our research group.<sup>50</sup> The purity of all the compounds was confirmed by ultraperformance liquid chromatography (UPLC) before any biological studies (spectra given in the Supporting Information). The fresh stock solution of all the compounds was made to be 5 mg/mL for each compound and was dissolved in 1 mL of the DMSO (molecular biology grade) solvent.

**5.2. Antibacterial Activity.** **5.2.1. Culture Preparation and Maintenance.** Five bacterial strains viz. *S. pneumoniae* (MTCC 655), *E. faecalis* (MTCC 439), *P. aeruginosa* (ATCC 2453), *S. typhimurium* (MTCC 3224), and *E. coli* (ATCC 25922) were streaked on nutrient agar plates and kept in an incubator overnight at 37 °C. A pure and single colony of each isolate was picked and inoculated into the nutrient broth and cultured in an incubator shaker overnight (Orbitech).

**5.2.2. Minimum Inhibitory Concentration (MIC) Determination.** To evaluate the MIC of the test compounds, the standard protocol recommended by the National Committee for Clinical Laboratory Standards (NCCLS) was followed. The test compounds (**OX1–OX27**) were studied for their antibacterial activity against two Gram-positive strains (*S. pneumoniae* and *E. faecalis*) and three Gram-negative strains (*S. typhimurium*, *P. aeruginosa*, and *E. coli*) using the conventional broth dilution method. The MIC values were calculated and compared with CIP and AMP as the reference antibiotics. The stock solution (5 mg/mL) of the standard drug (AMP and CIP) and synthesized compounds (**OX1–OX27**) was prepared in DMSO (molecular biology grade). To acquire the requisite concentrations of 500, 250, 125, 62.50, 31.25, 15.62, 7.81, 3.90, 1.95, 0.97, 0.48, and 0.24  $\mu\text{g}/\text{mL}$ , the progressive serial broth dilution method was used. A positive and a negative control were also taken in the experiment. The cultures were incubated at 37 °C for 24 h and then compared with blank in terms of turbidity caused by the microbial growth.

**5.2.3. Disk Diffusion Assay.** The disk diffusion assay was performed using aforesaid strains for the selected compounds **OX7** and **OX11**, which may have antimicrobial potential as they showed a low MIC value among tested compounds against the bacterial isolates.<sup>51</sup> The bacteria were cultivated overnight at 37 °C after being inoculated in a liquid broth medium. Approximately,  $10^5$  cells/mL was taken from that liquid broth medium and placed into Petri plates (Tarsons) after being inoculated into a molten nutritional agar medium. After solidification, sterilized 4 mm diameter disks of Whatman paper were placed on solid agar at an appropriate distance. Different concentrations of compounds, i.e., half MIC, MIC, and double MIC, were placed on the disks. For the positive and negative control, the standard drug and DMSO were applied onto the disks, respectively, while one disk was left blank for comparison. It was then kept in the incubator for 24 h at 37 °C. After 24 h, the diameter of the zone of inhibition



(ZOI) was accurately measured in millimeters, and the ZOI values of the positive and negative controls were compared.

**5.2.4. Growth Kinetics Assay.** The Gram-positive and Gram-negative strains of *S. pneumoniae* and *E. coli* cells were revived by sub-culture on the nutrient agar plate, respectively. An inoculum was then transferred into the liquid nutrient broth and before use; the cells were grown for 24 h at 37 °C to get a fresh culture. The growth kinetic assay was performed according to Saigal et al.<sup>5</sup> A graph was plotted between the O.D. and time duration (in h), and the effect of OX7 and OX11 on the growth of test organisms was determined.

**5.2.5. Time Kill Curve Study.** Time kill curves were examined to check the bacteriostatic/bactericidal effect of the compounds OX7 and OX11. *S. pneumoniae* and *E. coli* strains were used in this study. A control was also used to monitor the extent of full growth. The fresh culture ( $\sim 2 \times 10^6$  cells) of test organisms was inoculated in freshly prepared media. These cells were then treated to the test chemicals at MIC and 4MIC doses. For the time kill curve study, the protocol given by Saigal et al. was followed.<sup>5</sup>

**5.2.6. Synergistic Antibacterial Activity.** The synergistic activity of the test compounds OX7 and OX11 with standard drugs CIP and MP was determined using the microdilution checkerboard method.<sup>52</sup> CIP and AMP were serially diluted in columns from 8, 4, 2, 1, 0.5, 0.25, 0.125, and 0.062 and 10, 5, 2.5, 1.25, 0.625, 0.312, 0.156, and 0.078  $\mu\text{g}/\text{mL}$ , respectively, while test compounds were diluted in rows from 16, 8, 4, 2, 1, 0.5, 0.25, and 0.125  $\mu\text{g}/\text{mL}$  in a 96-microwell plate to obtain large numbers of combinations. The plates were inoculated with 100  $\mu\text{L}$  of the freshly prepared culture of *S. pneumoniae* or *E. coli* cells. After incubation, the combinatorial MIC value was evaluated at which no visible growth appeared. Using the equation (eq 1) given below, the synergy of compounds in terms of FICI (fractional inhibitory concentration index) was calculated

$$\text{FICI} = \frac{\text{MIC of drug A in combination with B}}{\text{MIC of drug A alone}} + \frac{\text{MIC of drug B in combination with A}}{\text{MIC of drug B alone}} \quad (1)$$

**5.3. Assessment of Biofilm Disruption.** **5.3.1. XTT Assay.** To observe the effect of compounds OX7 and OX11 on the metabolic activity of biofilm formation in the tested bacterial strains, the XTT (2,3-bis(2-methoxy-4-nitro-5-sulphophenyl)-2H-tetrazolium-5-carboxanilide) assay was conducted on *E. coli* and *S. pneumoniae* strains, with slight modifications as the previously reported method.<sup>5</sup> Briefly, 100  $\mu\text{L}$  of sterile nutrient broth was poured in the 96-well microtiter plate, inoculated with desired bacterial strains, and incubated at 37 °C for 24 h to allow biofilm formation. After incubation, the medium was discarded gently followed by gentle washing with PBS. Then, the fresh medium containing various concentrations of test compounds (64–0.5  $\mu\text{g}/\text{mL}$ ) was poured gently into each well and further incubated for 24 h at 37 °C. After incubation, the medium was evacuated and the non-adherent cells were cleaned using PBS. In each well, 50  $\mu\text{L}$  of XTT salt solution (HiMedia) and the plates were incubated in the dark for 90 min at 37 °C. Bacterial dehydrogenase converts XTT tetrazolium salt to XTT formazan, which causes a colorimetric change (turns orange) and has been related to cell survival. These colorimetric variations were determined by taking their optical densities at

490 nm on a spectrophotometer.<sup>53</sup> The % inhibition data was further interpreted from dose–response curves.

**5.3.2. Visualization of Biofilm Disruption by Scanning Electron Microscopic (SEM) Analysis.** The ability of the selected compounds OX7 and OX11 to disrupt biofilm formation was visualized by SEM analysis using *E. coli* cells by using a previously described protocol.<sup>5</sup> Test compounds were added in the plate and again incubated for the next 24 h at 37 °C. Samples were again washed with PBS and dried to examine under scanning electron microscopy.<sup>54</sup>

**5.4. In Vitro (Hemolytic and MTT Assay) and In Vivo (G. mellonella Larvae) Toxicity Studies of Test Compounds.**

**5.4.1. Hemolytic Assay.** The hemolytic activity of the compounds OX7 and OX11 was studied using human red blood cells (*hRBCs*).<sup>55</sup> The procedures used to perform the hemolytic study were similar to those reported earlier.<sup>56</sup>

% hemolysis was calculated from the following equation (eq 2).

$$\begin{aligned} \% \text{ hemolysis} = & [(A_{450} \text{ of the test compound treated sample} \\ & - A_{450} \text{ of the buffer treated sample}) \\ & \div (A_{450} \text{ of the 1\% Triton X-100} \\ & \text{treated sample} - A_{450} \\ & \text{of the buffer treated sample})] - 100 \quad (2) \end{aligned}$$

**5.4.2. MTT Assay.** To confirm the cytotoxic effect of selected compounds, the MTT assay was also performed following the encouraging results of the hemolytic assay. A typical MTT (3-(4,5-dimethylthiazol-2-yl)-2,5-diphenyl tetrazolium bromide) assay was used.<sup>57</sup> Cell line human embryonic kidney (HEK293) cells are widely used in cell biological research because of their consistent growth and inclination for transfection.<sup>58–60</sup> HEK293 cells were maintained and cultured in Dulbecco's modified Eagle's medium (DMEM) media enriched with 10% heat inactivated fetal bovine serum (FBS) and 1% penicillin and streptomycin solution in a humidified incubator (5% CO<sub>2</sub>) in T-25 flasks at 37 °C. Approximately  $2 \times 10^4$  cells (150  $\mu\text{L}$ ) were seeded per well in a 96-well plate and incubated for 24 h before treatment. After a day, cells were treated with increasing concentrations (0–250  $\mu\text{M}$ ) of each test compound in 200  $\mu\text{L}$  as the final volume at 37 °C for 48 h in a CO<sub>2</sub> incubator. Further assessment of the cytotoxicity was determined as mentioned by Uddin et al.<sup>61</sup> The control cells were treated with cell culture media only, and to nullify the effect of respective DMSO concentration, the cells were correspondingly treated with DMSO and subtracted from the respective compound-treated well readings. The percent of viable cells was determined and shown as a function of compound concentration.<sup>62</sup>

**5.4.3. In Vivo Toxicity Evaluation of Lead Compound OX11 on G. mellonella Larvae.** *In vivo* activity of OX11 was assessed in *G. mellonella* larvae, as previously described.<sup>63</sup> Larvae were inoculated with 20  $\mu\text{L}$  of OX11 solutions (7, 31, 62, or 125  $\mu\text{g}/\text{mL}$ ) and incubated in the dark for 24 h at 30 °C. The effect of the compound on hemocyte density was assessed as described.<sup>63</sup>

**5.5. TEM (Transmission Electron Microscopy) Analysis.** The morphology of *E. coli* cells, both treated (with OX11) and untreated, was examined by TEM analysis according to the standard protocol.<sup>64</sup> First of all, the mid-log phase *E. coli* cells were harvested and then treated to MIC



concentration of OX11. Afterward, washing of cells was done three times with PBS solution and fixed in 2.5% glutaraldehyde in phosphate/magnesium buffer overnight. By using 0.1 M sodium phosphate buffer (pH 6.0), the cells were washed twice for 15 min and cells were fixed in 2% osmium tetroxide for 2 h. After 2 h, cells were again washed twice in distilled water for 15 min and then *en bloc* stained for 30 min with 1% aqueous uranyl acetate. Cells were dehydrated in 95 and 100% ethanol after two more washing. The cells were then treated to propylene oxide for 2–10 min before being infiltrated for 1 h in a 1:1 propylene/epoxy embedding medium (Epon) combination and then overnight in fresh Epon. The ultrathin sections were cut after polymerization for 48 h at 60 °C using a microtome (Leica EM UC6) and transferred to a copper grid. After staining with a saturated solution of uranyl acetate in 50% alcohol, the samples were stained with lead citrate. These samples were washed three times in Milli-Q (MQ) water and dried by touching gently with Whatman filter paper. These thin sections were then examined with a FEI Tecnai G2 at 200 KV.

### 5.6. Confocal Laser Scanning Microscopic (CLSM)

**Analysis.** The lead compound OX11 was analyzed through CLSM to determine its effect on *E. coli* cells. The bacterial cells were stained using DAPI (4',6-diamidino-2-phenylindole), which is a fluorescent dye that binds tightly to the DNA's A-T rich region and emits blue fluorescence at 461 nm as emission spectra, upon excitation at 358 nm. The log-phase cells of *E. coli* were harvested by centrifugation for 15 min and washed twice with PBS buffer solution and further examined as mentioned previously.<sup>5</sup>

**5.7. Effect of the Lead Compound (OX11) on Resistant Bacterial Strains.** Based on the above pharmacological investigations, OX11 was found to be the promising antibacterial agent among all the tested compounds. The MIC of OX11 was determined against 19 different environmental isolates of *E. coli*, two strains of *K. pneumoniae*, and one strain each of *Acinetobacter* sp., *K. georgiana*, and *C. werkmanii*.<sup>30,31</sup> These environmental isolates were taken from the River Yamuna Delhi stretch (India) and drain effluent water of the Ghazipur Slaughter House (India). Some of these environmental isolates are multidrug resistant (MDR) phenotypes. Details of their resistance pattern against different antibiotics are given in Table 8. The studies on the synergistic effect (with AMP and sulfamethoxazole) were performed using a previously mentioned protocol.<sup>51</sup> Because of the structural similarities with OX11, we included the sulfamethoxazole (SMX) antibiotic in our study on resistant strains for comparison.

### 5.8. Human Serum Albumin (HSA) Binding Study.

UV-vis, fluorescence, synchronous, and CD spectroscopic techniques were employed to study the binding between HSA and OX11. The UV-vis spectra of HSA (5 μM) in the presence and absence of various concentrations of OX11 (0.1–6.8 μM) were recorded using an Analytik Jena Specord-250 spectrophotometer (USA) using a 1.0 cm cell at 298 K. The binding constant ( $K_b$ ) was also analyzed using the double reciprocal plot between  $1/A_0 - A_{vs} 1/[OX11]$  by eq 3.<sup>36</sup>

$$\frac{1}{A_0 - A} = \frac{1}{A_0} + \frac{1}{KA_0[C]} \quad (3)$$

Further, to confirm the quenching mechanism and the binding forces involved in complexation, fluorescence spectroscopy was employed. The fluorescence spectra of HSA (5 μM) in the presence and absence of different concentrations of

**Table 8. Phenotype and Resistance Pattern against Different Antibiotics of Environmental Isolates<sup>30,31a</sup>**

bacterial isolate code	strain	resistant	phenotype
AE-9	<i>E. coli</i>	AMP, AT, CTN, CXM, CZ, ETP, CIP, RIF	MDR
AE-27	<i>E. coli</i>	AMP, A/S, AT, CTN, CXM, CZ, ETP, IPM, CIP, LE, OF, RIF	MDR
AE-44	<i>E. coli</i>	AMP, A/S, AT, CTN, CXM, CZ, ETP, CIP, LE, OF, RIF	MDR
AE-32	<i>E. coli</i>	AMP, A/S, AT, CTN, CXM, CZ, ETP, CIP, LE, OF, PB, TOB, TR	MDR
AE-17	<i>E. coli</i>	AMP, AT, CTN, CXM, CZ, ETP, CIP, RIF	MDR
AE-23	<i>E. coli</i>	AMP, CTN, CXM, CZ, ETP, RIF	MDR
AE-42	<i>E. coli</i>	AMP, A/S, AT, CTN, CXM, CZ, ETP, CIP, LE, RIF, TOB, TR	MDR
AE-21	<i>E. coli</i>	AMP, A/S, CXM	non-MDR
AE-31	<i>E. coli</i>	AMP, A/S, AT, CTN, CXM, CZ, ETP, IPM, CX, CIP, LE, OF, RIF, TE, AK, TOB	MDR
EC-36	<i>E. coli</i>	AMP, CTN	non-MDR
EC-2	<i>E. coli</i>	AMP, CTN, CXM, CZ, RIF	MDR
EC-3	<i>E. coli</i>	AMP, CTN, CXM, CZ, RIF	MDR
EC-6	<i>E. coli</i>	AMP, A/S, CTN, CXM, CZ, LE, CIP, OF, RIF, TE, TR	MDR
EC-25	<i>E. coli</i>	AMP, CTX	non-MDR
OB-18	<i>E. coli</i>	AMP, AT, CZ, ETP, RIF, TR	MDR
OB-6	<i>E. coli</i>	AMP, AT, CZ, ETP, RIF, TR	MDR
AE-2	<i>E. coli</i>	AMP, A/S, AT, CTN, CXM, CZ, ETP, CIP	MDR
OE-11	<i>E. coli</i>	CTX, AMP	non-MDR
EE-2	<i>E. coli</i>	CIP, LE, OF, RIF, AMP, CTN, CXM, CZ	MDR
EH-8	<i>Acinetobacter</i> sp.	AT, CTN, CX, CXM, CZ, ETP, CIP, PB, AK	MDR
KP	<i>K. pneumoniae</i>	AT, CTN, CXM, CZ, ETP, IPM, RIF, TE	MDR
EA-13	<i>K. pneumoniae</i>	CIP, OF, RIF, TR, AMP	MDR
SH-14	<i>K. georgiana</i>	CAZ, CTX, CTR	non-MDR
SH-52	<i>C. werkmanii</i>	CL, PB, TR, RIF, AT, ETP, CZ, CX, CAZ, CTX	MDR

<sup>a</sup>AMP: ampicillin, A/S: ampicillin/sulbactam, AT: aztreonam, CTN: cefotetan, CX: ceftiofloxacin, CTX: cefotaxime, CXM: cefuroxime, CZ: cefazolin, ETP: ertapenem, IPM: imipenem, CIP: ciprofloxacin, LE: levofloxacin, OF: ofloxacin, PB: pliximix B, RIF: rifampicin, TE: tetracyclin, AK: amikacin, TOB: tobramycin, TR: trimethoprim.

OX11 (0.1–6.8 μM) were recorded on a Cary Eclipse spectrofluorometer (Varian, USA) equipped with a 150 W xenon lamp at 298, 303, and 308 K using a quartz cuvette (1.0 cm) at 280 nm as the excitation wavelength. Temperature was maintained in the assays using a constant temperature cell holder coupled to a constant temperature water circulator (Varian, USA). In addition, synchronous spectra were obtained using the same spectrofluorometer. The difference between the excitation and emission ( $\Delta\lambda = \lambda_{em} - \lambda_{ex}$ ) wavelength was kept constant. The  $\Delta\lambda$  at 15 nm or 60 nm showed by synchronous fluorescence spectra gave characteristic information of tyrosine (Tyr) residues or tryptophan (Trp) residues with the excitation and emission slit widths at 5 nm. The quenching mechanism was determined according to the Stern–Volmer equation (eqs 4 and 5).<sup>65</sup>

$$\frac{F_0}{F} = 1 + K_{sv} [Q] \quad (4)$$

$$\log \frac{F_0 - F}{F} = \log K_a + n \log [Q] \quad (5)$$

where  $F_0$  and  $F$  represent the protein's relative fluorescence intensity in the presence and absence of the quencher OX11. The Stern–Volmer quenching constant is  $K_{sv}$ , and the molar concentration of OX11 is  $[Q]$ . The  $K_{sv}$  values were calculated using the slope of the HSA–OX11 system's Stern–Volmer plot. Also, the binding parameters such as the binding constant ( $K_b$ ) and the number of binding sites ( $n$ ) are calculated using eq 3 and thermodynamic parameters like enthalpy change ( $\Delta H$ ), entropy change ( $\Delta S$ ), and Gibbs energy change ( $\Delta G$ ) were also determined by carefully analyzing the fluorescence data according to the thermodynamic equations (eqs 6 and 7).<sup>66</sup>

$$\ln K = \frac{\Delta H}{RT} + \frac{\Delta S}{R} \quad (6)$$

$$\Delta G = \Delta H - T\Delta S \quad (7)$$

Also, three-dimensional fluorescence was noted on the same instrument. The excitation wavelength was set at 200 nm, and emission was recorded between 200 and 400 with an interval of 10 nm. The CD spectra were recorded on a JASCO J-815 spectropolarimeter at 298 K with a cell holder (thermostatically controlled) attached to a Neslab RTE-110 water bath with an accuracy of  $\pm 0.1$  K. The CD instrument was calibrated using a quartz cuvette of 0.1 cm path length at 298 K. The spectra were recorded in the far UV range from 200 to 250 nm at a scan rate of 50 nm/min, and each spectrum is the average of three scans with a full-scale sensitivity of 10mdeg. The concentration of HSA used was 5  $\mu$ M. The  $\alpha$ -helical contents of free and combined protein were calculated from mean residue ellipticity (MRE) values at 208 nm by using eqs 8 and 9.<sup>67</sup>

$$[\theta]_i = \frac{M_o[\theta]}{10IC} \quad (8)$$

$$[\alpha] = \frac{-MRE_{208} - 4000}{33,000 - 4000} \quad (9)$$

## ■ ASSOCIATED CONTENT

### SI Supporting Information

The Supporting Information is available free of charge at <https://pubs.acs.org/doi/10.1021/acsomega.1c03379>.

Supplementary data includes spectral data of the test compounds OX7 and OX11 and images of agar plates showing the zone of inhibition (PDF)

## ■ AUTHOR INFORMATION

### Corresponding Authors

Qazi Mohd. Rizwanul Haque – Microbiology Research Laboratory, Department of Biosciences, Jamia Millia Islamia, New Delhi 110025, India; Email: [qhaque@jmi.ac.in](mailto:qhaque@jmi.ac.in)

Mohammad Abid – Medicinal Chemistry Laboratory, Department of Biosciences, Jamia Millia Islamia, New Delhi 110025, India; [orcid.org/0000-0002-0507-8451](https://orcid.org/0000-0002-0507-8451); Phone: +91-8750295095; Email: [mabid@jmi.ac.in](mailto:mabid@jmi.ac.in); Fax: +91-11-26980229

## Authors

Asghar Ali – Microbiology Research Laboratory, Department of Biosciences, Jamia Millia Islamia, New Delhi 110025, India

Phool Hasan – Medicinal Chemistry Laboratory, Department of Biosciences, Jamia Millia Islamia, New Delhi 110025, India

Mohammad Irfan – Medicinal Chemistry Laboratory, Department of Biosciences, Jamia Millia Islamia, New Delhi 110025, India

Amad Uddin – Medicinal Chemistry Laboratory, Department of Biosciences, Jamia Millia Islamia, New Delhi 110025, India

Ashba Khan – Medicinal Chemistry Laboratory, Department of Biosciences, Jamia Millia Islamia, New Delhi 110025, India

Juhi Saraswat – Biophysical Chemistry Laboratory, Centre for Interdisciplinary Research in Basic Sciences, Jamia Millia Islamia, New Delhi 110025, India

Ronan Maguire – Department of Biology, Maynooth University, Maynooth ABC127, Ireland

Kevin Kavanagh – Department of Biology, Maynooth University, Maynooth ABC127, Ireland; [orcid.org/0000-0003-3186-0292](https://orcid.org/0000-0003-3186-0292)

Rajan Patel – Biophysical Chemistry Laboratory, Centre for Interdisciplinary Research in Basic Sciences, Jamia Millia Islamia, New Delhi 110025, India; [orcid.org/0000-0002-3811-2898](https://orcid.org/0000-0002-3811-2898)

Mukesh C. Joshi – Motilal Nehru College, University of Delhi, New Delhi 110021, India

Amir Azam – Department of Chemistry, Jamia Millia Islamia, New Delhi 110025, India; [orcid.org/0000-0002-8893-0450](https://orcid.org/0000-0002-8893-0450)

Mohd. Mohsin – Metabolic Engineering Laboratory, Department of Biosciences, Jamia Millia Islamia, New Delhi 110025, India; [orcid.org/0000-0002-4127-5970](https://orcid.org/0000-0002-4127-5970)

Complete contact information is available at:

<https://pubs.acs.org/10.1021/acsomega.1c03379>

## Author Contributions

○A.A. and P.H. are equal contributors. M.A. designed the project and optimized the experiments. P.H. synthesized the compounds. A.A., M.I., A.U., and A.K. screened and performed all the biological experiments. R.M. and K.K. performed *in vivo* toxicological studies using *G. mellonella*. J.S. and R.P. performed HSA binding studies. M.A., A.A., M.I., A.U., and A.K. interpreted the data and wrote the manuscript. M.A., A.A., M.M., and M.C.J. edited the final manuscript. M.A. provided funding acquisition and aided administrative processing. All the authors approved and reviewed the final version of the manuscript.

## Notes

The authors declare no competing financial interest.

## ■ ACKNOWLEDGMENTS

M.A. gratefully acknowledges the financial support in the form of the Core Research Grant from the Science & Engineering Research Board (SERB), Government of India (file no. CRG/2018/003967). A.U. is a recipient of the Senior Research Fellowship from ICMR (Fellowship/48/2019-ECD-II). Authors also acknowledge SAIF, AIIMS, New Delhi, for providing scanning and transmission electron microscopic facilities.

## REFERENCES

- (1) <https://News.Un.Org/En/Story/2016/09/539912-Un-Global-Leaders-Commit-Act-Antimicrobial-Resistance>.
- (2) MacGowan, A.; Macnaughton, E. Antibiotic Resistance. *Medicine* **2017**, *45*, 622–628.
- (3) Burt, S. A.; Ojo-Fakunle, V. T. A.; Woertman, J.; Veldhuizen, E. J. A. The Natural Antimicrobial Carvacrol Inhibits Quorum Sensing in *Chromobacterium Violaceum* and Reduces Bacterial Biofilm Formation at Sub-Lethal Concentrations. *PLoS One* **2014**, *9*, No. e93414.
- (4) Lewis, K. Programmed Death in Bacteria. *Microbiol. Mol. Biol. Rev.* **2000**, *64*, 503–514.
- (5) Saigal; Irfan, M.; Khan, P.; Abid, M.; Khan, M. M. Design, Synthesis, and Biological Evaluation of Novel Fused Spiro-4H-Pyran Derivatives as Bacterial Biofilm Disruptor. *ACS Omega* **2019**, *4*, 16794–16807.
- (6) Habib, F.; Alam, S.; Hussain, A.; Aneja, B.; Irfan, M.; Alajmi, M. F.; Hasan, P.; Khan, P.; Rehman, M. T.; Noman, O. M.; Azam, A.; Abid, M. Biofilm Inhibition and DNA Binding Studies of Isoxazole-Triazole Conjugates in the Development of Effective Anti-Bacterial Agents. *J. Mol. Struct.* **2020**, *1201*, 127144.
- (7) Porta, F.; Facchetti, G.; Ferri, N.; Gelain, A.; Meneghetti, F.; Villa, S.; Barlocco, D.; Masciocchi, D.; Asai, A.; Miyoshi, N.; Marchianò, S.; Kwon, B. M.; Jin, Y.; Gandin, V.; Marzano, C.; Rimoldi, I. An in Vivo Active 1,2,5-Oxadiazole Pt(II) Complex: A Promising Anticancer Agent Endowed with STAT3 Inhibitory Properties. *Eur. J. Med. Chem.* **2017**, *131*, 196–206.
- (8) Ragab, F. A. F.; Abou-Seri, S. M.; Abdel-Aziz, S. A.; Alfayomy, A. M.; Abolmagd, M. Design, Synthesis and Anticancer Activity of New Monastrol Analogues Bearing 1,3,4-Oxadiazole Moiety. *Eur. J. Med. Chem.* **2017**, *138*, 140–151.
- (9) Tok, F.; Kocyigit-Kaymakcioglu, B.; Tabanca, N.; Estep, A. S.; Gross, A. D.; Geldenhuys, W. J.; Becnel, J. J.; Bloomquist, J. R. Synthesis and Structure–Activity Relationships of Carbohydrazides and 1,3,4-Oxadiazole Derivatives Bearing an Imidazolidine Moiety against the Yellow Fever and Dengue Vector, *Aedes Aegypti*. *Pest Manage. Sci.* **2018**, *74*, 413–421.
- (10) Patel, N. B.; Patel, J. N.; Purohit, A. C.; Patel, V. M.; Rajani, D. P.; Moo-Puc, R.; Lopez-Cedillo, J. C.; Nogueira-Torres, B.; Rivera, G. In Vitro and in Vivo Assessment of Newer Quinoxaline–Oxadiazole Hybrids as Antimicrobial and Antiprotozoal Agents. *Int. J. Antimicrob. Agents* **2017**, *50*, 413–418.
- (11) Thakkar, S. S.; Thakor, P.; Ray, A.; Doshi, H.; Thakkar, V. R. Benzothiazole Analogues: Synthesis, Characterization, MO Calculations with PM6 and DFT, in Silico Studies and in Vitro Antimalarial as DHFR Inhibitors and Antimicrobial Activities. *Bioorg. Med. Chem.* **2017**, *25*, 5396–5406.
- (12) Mihajlović, N.; Marković, V.; Matić, I. Z.; Stanisavljević, N. S.; Jovanović, Ž. S.; Trifunović, S.; Joksović, L. Synthesis and Antioxidant Activity of 1,3,4-Oxadiazoles and Their Diacylhydrazine Precursors Derived from Phenolic Acids. *RSC Adv.* **2017**, *7*, 8550–8560.
- (13) Sauer, A. C.; Leal, J. G.; Stefanello, S. T.; Leite, M. T. B.; Souza, M. B.; Soares, F. A. A.; Rodrigues, O. E. D.; Dornelles, L. Synthesis and Antioxidant Properties of Organosulfur and Organoselenium Compounds Derived from 5-Substituted-1,3,4-Oxadiazole/Thiadiazole-2-Thiols. *Tetrahedron Lett.* **2017**, *58*, 87–91.
- (14) Wang, P. Y.; Zhou, L.; Zhou, J.; Wu, Z. B.; Xue, W.; Song, B. A.; Yang, S. Synthesis and Antibacterial Activity of Pyridinium-Tailored 2,5-Substituted-1,3,4-Oxadiazole Thioether/Sulfoxide/Sulfone Derivatives. *Bioorg. Med. Chem. Lett.* **2016**, *26*, 1214–1217.
- (15) Zhang, T.-T.; Wang, P.-Y.; Zhou, J.; Shao, W.-B.; Fang, H. S.; Zhou, X.; Wu, Z.-B. Antibacterial and Antifungal Activities of 2-(Substituted Ether)-5-(1-Phenyl-5-(Trifluoromethyl)-1H-Pyrazol-4-Yl)-1,3,4-Oxadiazole Derivatives. *J. Heterocycl. Chem.* **2017**, *54*, 2319–2325.
- (16) Gan, X.; Hu, D.; Chen, Z.; Wang, Y.; Song, B. Synthesis and Antiviral Evaluation of Novel 1,3,4-Oxadiazole/Thiadiazole-Chalcone Conjugates. *Bioorg. Med. Chem. Lett.* **2017**, *27*, 4298–4301.
- (17) Benmansour, F.; Trist, I.; Coutard, B.; Decroly, E.; Querat, G.; Brancala, A.; Barral, K. Discovery of Novel Dengue Virus NS5 Methyltransferase Non-Nucleoside Inhibitors by Fragment-Based Drug Design. *Eur. J. Med. Chem.* **2017**, *125*, 865–880.
- (18) Rathore, A.; Sudhakar, R.; Ahsan, M. J.; Ali, A.; Subbarao, N.; Jadav, S. S.; Umar, S.; Yar, M. S. In Vivo Anti-Inflammatory Activity and Docking Study of Newly Synthesized Benzimidazole Derivatives Bearing Oxadiazole and Morpholine Rings. *Bioorg. Chem.* **2017**, *70*, 107.
- (19) Liu, Q.; Zhu, R.; Gao, S.; Ma, S. H.; Tang, H. J.; Yang, J. J.; Diao, Y. M.; Wang, H. L.; Zhu, H. J. Structure-Based Bioisosterism Design, Synthesis, Insecticidal Activity and Structure–Activity Relationship (SAR) of Anthranilic Diamide Analogues Containing 1,2,4-Oxadiazole Rings. *Pest Manage. Sci.* **2017**, *73*, 917–924.
- (20) Yoshino, H.; Ueda, N.; Nijima, J.; Sugumi, H.; Kotake, Y.; Koyanagi, N.; Yoshimatsu, K.; Asada, M.; Watanabe, T.; Nagasu, T.; Tsukahara, K.; Iijima, A.; Kitoh, K. Novel Sulfonamides as Potential, Systemically Active Antitumor Agents. *J. Med. Chem.* **1992**, *35*, 2496–2497.
- (21) Li, J. J.; Anderson, G. D.; Burton, E. G.; Cogburn, J. N.; Collins, J. T.; Garland, D. J.; Gregory, S. A.; Huang, H. C.; Isakson, P. C.; Koboldt, C. M.; Logusch, E. W.; Norton, M. B.; Perkins, W. E.; Reinhard, E. J.; Seibert, K.; Veenhuizen, A. W.; Zhang, Y.; Reitz, D. B. 1,2-Diarylcyclopentenes as Selective Cyclooxygenase-2 Inhibitors and Orally Active Anti-Inflammatory Agents. *J. Med. Chem.* **1995**, *38*, 4570–4578.
- (22) Renzi, G.; Scozzafava, A.; Supuran, C. T. Carbonic Anhydrase Inhibitors: Topical Sulfonamide Antiglaucoma Agents Incorporating Secondary Amine Moieties. *Bioorg. Med. Chem. Lett.* **2000**, *10*, 673–676.
- (23) Maren, T. H. Relations between Structure and Biological Activity of Sulfonamides. *Annu. Rev. Pharmacol. Toxicol.* **1976**, *16*, 309–327.
- (24) Yamasaki, K.; Chuang, V. T. G.; Maruyama, T.; Otagiri, M. Albumin-Drug Interaction and Its Clinical Implication. *Biochim. Biophys. Acta, Gen. Subj.* **2013**, *1830*, 5435–5443.
- (25) Jusko, W. J.; Gretch, M. Plasma and Tissue Protein Binding of Drugs in Pharmacokinetics. *Drug Metab. Rev.* **1976**, *5*, 43–140.
- (26) Vallner, J. J. Binding of Drugs by Albumin and Plasma Protein. *J. Pharm. Sci.* **1977**, *66*, 447–465.
- (27) Otagiri, M. Study on Binding of Drug to Serum Protein. *Yakugaku Zasshi* **2009**, *129*, 413–425.
- (28) Meyer, M. C.; Guttman, D. E. The Binding of Drugs by Plasma Proteins. *J. Pharm. Sci.* **1968**, *57*, 895–918.
- (29) Marques, M. B.; Brookings, E. S.; Moser, S. A.; Sonke, P. B.; Waites, K. B. Comparative in Vitro Antimicrobial Susceptibilities of Nosocomial Isolates of *Acinetobacter Baumannii* and Synergistic Activities of Nine Antimicrobial Combinations. *Antimicrob. Agents Chemother.* **1997**, *41*, 881–885.
- (30) Ali, A.; Sultan, I.; Mondal, A. H.; Siddiqui, M. T.; Gogry, F. A.; Haq, Q. M. R. Lentic and Effluent Water of Delhi-NCR: A Reservoir of Multidrug-Resistant Bacteria Harboring BlaCTX-M, Bla TEM and BlaSHV Type ESBL Genes. *J. Water Health* **2021**, *592*.
- (31) Azam, M.; Kumar, V.; Siddiqui, K.; Jan, A. T.; Sabir, J. S. M.; Rather, I. A.; Rehman, S.; Haq, Q. M. R. Pharmaceutical Disposal Facilitates the Mobilization of Resistance Determinants among Microbiota of Polluted Environment. *Saudi Pharm. J.* **2020**, *28*, 1626–1634.
- (32) Patel, R.; Maurya, N.; Parray, M. u. d.; Farooq, N.; Siddique, A.; Verma, K. L.; Dohare, N. Esterase Activity and Conformational Changes of Bovine Serum Albumin toward Interaction with Mephedrone: Spectroscopic and Computational Studies. *J. Mol. Recognit.* **2018**, *31*, No. e2734.
- (33) Ross, P. D.; Subramanian, S. Thermodynamics of Protein Association Reactions: Forces Contributing to Stability. *Biochemistry* **1981**, *20*, 3096–3102.
- (34) Maurya, N.; Maurya, J. K.; Singh, U. K.; Dohare, R.; Zafaryab, M.; Moshahid Alam Rizvi, M.; Kumari, M.; Patel, R. In Vitro Cytotoxicity and Interaction of Noscapine with Human Serum Albumin: Effect on Structure and Esterase Activity of HSA. *Mol. Pharmaceutics* **2019**, *16*, 952–966.



- (35) Sharma, T.; Dohare, N.; Kumari, M.; Singh, U. K.; Khan, A. B.; Borse, M. S.; Patel, R. Comparative Effect of Cationic Gemini Surfactant and Its Monomeric Counterpart on the Conformational Stability and Activity of Lysozyme. *RSC Adv.* **2017**, *7*, 16763–16776.
- (36) Parray, M. d.; Maurya, N.; Ahmad Wani, F.; Borse, M. S.; Arfin, N.; Ahmad Malik, M.; Patel, R. Comparative Effect of Cationic Gemini Surfactant and Its Monomeric Counterpart on the Conformational Stability of Phospholipase A2. *J. Mol. Struct.* **2019**, *1175*, 49–55.
- (37) Dohare, N.; ud din Parray, M.; Siddiquee, M. A.; Khan, A. B.; Alzahrani, K. A.; Alshehri, A. A.; Malik, M. A.; Patel, R. Effect of Adiphenine Hydrochloride on the Structure of Bovine Serum Albumin: Spectroscopic and Docking Study. *J. Mol. Struct.* **2020**, *1201*, 127168.
- (38) Singh, U. K.; Kumari, M.; Wani, F. A.; Parray, M. u. d.; Saraswat, J.; Venkatesu, P.; R, P. Refolding of Acid Denatured Cytochrome c by Anionic Surface-Active Ionic Liquid: Choice of Anion Plays Key Role in Refolding of Proteins. *Colloids Surf, A* **2019**, *582*, 123872.
- (39) Davey, M. S.; Tyrrell, J. M.; Howe, R. A.; Walsh, T. R.; Moser, B.; Toleman, M. A.; Eberl, M. A Promising Target for Treatment of Multidrug-Resistant Bacterial Infections. *Antimicrob. Agents Chemother.* **2011**, *55*, 3635–3636.
- (40) Bassetti, M.; Peghin, M.; Vena, A.; Giacobbe, D. R. Treatment of Infections Due to MDR Gram-Negative Bacteria. *Front. Med.* **2019**, *6*, 74.
- (41) WHO *Antimicrobial Resistance*; World Health Organization: 2020.
- (42) Frieden, T. *Antibiotic Resistance Threats in the United States*; Centers for Disease Control and Prevention: 2013.
- (43) Sharom, J. R.; Bellows, D. S.; Tyers, M. From Large Networks to Small Molecules. *Curr. Opin. Chem. Biol.* **2004**, *8*, 81–90.
- (44) Kaelin, W. G., Jr. The Concept of Synthetic Lethality in the Context of Anticancer Therapy. *Nat. Rev. Cancer* **2005**, *5*, 689–698.
- (45) Keith, C. T.; Borisy, A. A.; Stockwell, B. R. Multicomponent Therapeutics for Networked Systems. *Nat. Rev. Drug Discovery* **2005**, *4*, 71–78.
- (46) Davies, D. Understanding Biofilm Resistance to Antibacterial Agents. *Nat. Rev. Drug Discovery* **2003**, *2*, 114–122.
- (47) Fux, C. A.; Costerton, J. W.; Stewart, P. S.; Stoodley, P. Survival Strategies of Infectious Biofilms. *Trends Microbiol.* **2005**, *34*.
- (48) Hervé, F.; Urien, S.; Albengres, E.; Duché, J.-C.; Tillement, J.-P. Drug Binding in Plasma. A Summary of Recent Trends in the Study of Drug and Hormone Binding. *Clin. Pharmacokinet.* **1994**, *26*, 44–58.
- (49) Goodman, L. S. *Goodman and Gilman's the Pharmacological Basis of Therapeutics*; McGraw-Hill: 1996, 1549.
- (50) Shamsi, F.; Hasan, P.; Queen, A.; Hussain, A.; Khan, P.; Zeya, B.; King, H. M.; Rana, S.; Garrison, J.; Alajmi, M. F.; Rizvi, M. M. A.; Zahid, M.; Hassan, M. I.; Abid, M. Synthesis and SAR Studies of Novel 1,2,4-Oxadiazole-Sulfonamide Based Compounds as Potential Anticancer Agents for Colorectal Cancer Therapy. *Bioorg. Chem.* **2020**, *98*, 103754.
- (51) National Antimicrobial Resistance Monitoring System *Enteric Bacteria*; CDC; USA, 2002.
- (52) Rand, K. H.; Houck, H. J.; Brown, P.; Bennett, D. Reproducibility of the Microdilution Checkerboard Method for Antibiotic Synergy. *Antimicrob. Agents Chemother.* **1993**, *37*, 613–615.
- (53) Felton, L.; Kauffmann, G.; Prescott, B.; Ottinger, B. Studies on the Mechanism of the Immunological Paralysis Induced in Mice by Pneumococcal Polysaccharides. *J. Immunol.* **1995**, *74*, 17–26.
- (54) Antoci, V., Jr.; Adams, C. S.; Parvizi, J.; Davidson, H. M.; Composto, R. J.; Freeman, T. A.; Wickstrom, E.; Ducheyne, P.; Jungkind, D.; Shapiro, I. M.; Hickok, N. J. The Inhibition of Staphylococcus Epidermidis Biofilm Formation by Vancomycin-Modified Titanium Alloy and Implications for the Treatment of Periprosthetic Infection. *Biomaterials* **2008**, *29*, 4684–4690.
- (55) Aneja, B.; Azam, M.; Alam, S.; Perwez, A.; Maguire, R.; Yadava, U.; Kavanagh, K.; Daniliuc, C. G.; Rizvi, M. M. A.; Haq, Q. M. R.; Abid, M. Natural Product-Based 1,2,3-Triazole/Sulfonate Analogues as Potential Chemotherapeutic Agents for Bacterial Infections. *ACS Omega* **2018**, *3*, 6912–6930.
- (56) Lathwal, A.; Ali, A.; Uddin, A.; Khan, N. S.; Sheehan, G.; Kavanagh, K.; Haq, Q. M. R.; Abid, M.; Nath, M. Assessment of Dihydro[1,3]Oxazine-Fused Isoflavone and 4-Thionoisoflavone Hybrids as Antibacterials. *ChemistrySelect* **2021**, *6*, 7505–7513.
- (57) Wani, F. A.; Amaduddin; Aneja, B.; Sheehan, G.; Kavanagh, K.; Ahmad, R.; Abid, M.; Patel, R. Synthesis of Novel Benzimidazolium Gemini Surfactants and Evaluation of Their Anti-Candida Activity. *ACS Omega* **2019**, *4*, 11871–11879.
- (58) Reddy, A. R. N.; Reddy, Y. N.; Krishna, D. R.; Himabindu, V. Multi Wall Carbon Nanotubes Induce Oxidative Stress and Cytotoxicity in Human Embryonic Kidney (HEK293) Cells. *Toxicology* **2010**, *272*, 11–16.
- (59) Su, Y.; Hu, M.; Fan, C.; He, Y.; Li, Q.; Li, W.; Wang, L. h.; Shen, P.; Huang, Q. The Cytotoxicity of CdTe Quantum Dots and the Relative Contributions from Released Cadmium Ions and Nanoparticle Properties. *Biomaterials* **2010**, *31*, 4829–4834.
- (60) Selvaraj, V.; Bodapati, S.; Murray, E.; Rice, K. M.; Winston, N.; Shokuhfar, T.; Zhao, Y.; Blough, E. Cytotoxicity and Genotoxicity Caused by Yttrium Oxide Nanoparticles in HEK293 Cells. *Int. J. Nanomed.* **2014**, *9*, 1379–1391.
- (61) Uddin, A.; Singh, V.; Irfan, I.; Mohammad, T.; Singh Hada, R.; Imtaiyaz Hassan, M.; Abid, M.; Singh, S. Identification and Structure–Activity Relationship (SAR) Studies of Carvacrol Derivatives as Potential Anti-Malarial against Plasmodium Falciparum Falcipain-2 Protease. *Bioorg. Chem.* **2020**, *103*, 104142.
- (62) Aneja, B.; Irfan, M.; Kapil, C.; Jairajpuri, M. A.; Maguire, R.; Kavanagh, K.; Rizvi, M. M. A.; Manzoor, N.; Azam, A.; Abid, M. Effect of Novel Triazole-Amino Acid Hybrids on Growth and Virulence of Candida Species: In Vitro and in Vivo Studies. *Org. Biomol. Chem.* **2016**, *14*, 10599–10619.
- (63) Fallon, J.; Kelly, J.; Kavanagh, K. Galleria Mellonella as a Model for Fungal Pathogenicity Testing. In *Host-Fungus Interactions*; Brand, A.; MacCallum, D. (Eds), Humana, Totowa, NJ, 2012, DOI: 10.1007/978-1-61779-539-8\_33.
- (64) Irfan, M.; Alam, S.; Manzoor, N.; Abid, M. Effect of Quinoline Based 1,2,3-Triazole and Its Structural Analogues on Growth and Virulence Attributes of Candida Albicans. *PLoS One* **2017**, *12*, No. e0175710.
- (65) Kumari, M.; Singh, U. K.; Khan, A. B.; Malik, M. A.; Patel, R. Effect of Bovine Serum Albumin on the Surface Properties of Ionic Liquid-Type Gemini Surfactant. *J. Dispersion Sci. Technol.* **2018**, *39*, 1462–1468.
- (66) Maurya, N.; Maurya, J. K.; Kumari, M.; Khan, A. B.; Dohare, R.; Patel, R. Hydrogen Bonding-Assisted Interaction between Amitriptyline Hydrochloride and Hemoglobin: Spectroscopic and Molecular Dynamics Studies. *J. Biomol. Struct. Dyn.* **2017**, *35*, 1367–1380.
- (67) Maurya, J. K.; Mir, M. U. H.; Maurya, N.; Dohare, N.; Ali, A.; Patel, R. A Spectroscopic and Molecular Dynamic Approach on the Interaction between Ionic Liquid Type Gemini Surfactant and Human Serum Albumin. *J. Biomol. Struct. Dyn.* **2016**, *34*, 2130–2145.